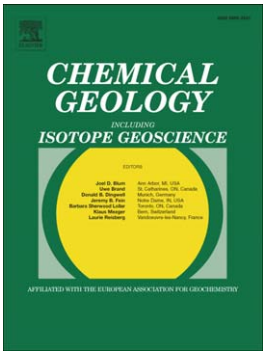

U-Pb LA-ICPMS dating using accessory mineral standards with variable common Pb

D.M. Chew, J.A. Petrus, B.S. Kamber

PII: S0009-2541(13)00510-X
DOI: doi: 10.1016/j.chemgeo.2013.11.006
Reference: CHEMGE 17075

To appear in: *Chemical Geology*

Received date: 29 June 2013
Revised date: 9 November 2013
Accepted date: 11 November 2013

Please cite this article as: Chew, D.M., Petrus, J.A., Kamber, B.S., U-Pb LA-ICPMS dating using accessory mineral standards with variable common Pb, *Chemical Geology* (2013), doi: 10.1016/j.chemgeo.2013.11.006

U-Pb LA-ICPMS dating using accessory mineral standards with variable common Pb

D.M. CHEW[1*], J.A. PETRUS[2], B.S. KAMBER[1]

[1]Dept. of Geology, Trinity College Dublin, Dublin 2, Ireland (*correspondence: chewd@tcd.ie, kamberbs@tcd.ie)

[2]Department of Earth Sciences, Laurentian University, Sudbury, Canada (jpetrus@laurentian.ca)

Abstract

Precise and accurate U–Pb LA-ICPMS dating of many U-bearing accessory minerals (e.g. apatite, allanite, titanite and rutile) is often compromised by common Pb. LA-ICPMS dating of these U-bearing accessory phases typically requires a matrix-matched standard, and data reduction is often complicated by *variable* incorporation of common Pb not only into the unknowns but particularly into the reference material. We present here a general approach to common Pb correction in U–Pb LA-ICP-MS dating using a modified version of the VizualAge U-Pb data reduction package for Iolite (VizualAge_UcomPbine). The key feature of the method is that it can correct for *variable* amounts of common Pb in any U-Pb accessory mineral *standard* as long as the standard is concordant in the U/Pb (and Th/Pb) systems following common Pb correction. Common Pb correction of the age standard can be undertaken using either the ^{204}Pb, ^{207}Pb or $^{208}Pb_{(no\ Th)}$ methods, and the approach can be applied to raw data files from all widely used modern multi-collector and single-collector ICPMS instruments.

VizualAge_UcomPbine first applies a common Pb correction to the user-selected age standard integrations and then fits session-wide "model" U-Pb fractionation curves to the time-resolved U-Pb standard data. This downhole fractionation model is applied to the unknowns and sample-standard bracketing (using a user-specified interpolation method) is used to calculate final isotopic ratios and ages. ^{204}Pb- and $^{208}Pb_{(no\ Th)}$-corrected concordia diagrams and ^{204}Pb-, ^{207}Pb- and $^{208}Pb_{(no\ Th)}$-corrected age channels can be calculated for user-specified initial Pb ratio(s). All other conventional common Pb correction methods (e.g. intercept or isochron methods on co-genetic analyses) can be performed offline.

The approach was tested on apatite and titanite age standards (for which there are independent constraints on the U-Pb crystallization age) using a Thermo Scientific iCAP-Qc (Q-ICP-MS) coupled to a Photon Machines Analyte Excite 193 nm ArF Excimer laser. Madagascar apatite, OLT1 titanite and R10 rutile were used as primary standards and were corrected for variable common Pb using the new VizualAge_UcomPbine DRS. The secondary Durango (31.44 ± 0.18 Ma) apatite standard yielded a U-Pb TW concordia intercept age of 31.97 ± 0.59 Ma (MSWD = 1.09; primary standard corrected by the ^{207}Pb-method) and a U-Pb concordia age of 31.82 ± 0.40 Ma (MSWD = 1.4; primary standard corrected by the ^{204}Pb-method). McClure Mountain (523.51 ± 1.47 Ma) yielded a U-Pb TW concordia intercept age of 524.5 ± 3.7 Ma (MSWD = 0.72) while the Fish Canyon Tuff (28.201 ± 0.046 Ma) and Khan (522.2 ± 2.2 Ma) titanite standards yielded U-Pb TW concordia intercept ages of 28.78 ± 0.41 Ma (MSWD = 1.4) and 520.9 ± 3.9 Ma (MSWD = 4.2) respectively. The suitability of the $^{208}Pb_{(no\ Th)}$-correction is demonstrated by the agreement between a U-Pb TW concordia intercept age of 452.6 ± 4.7 Ma (MSWD = 0.89) and a $^{208}Pb_{(no\ Th)}$-corrected TW concordia age of 448.6 ± 4.5 Ma (MSWD = 1.4) on a c. 450 Ma rutile which exhibits variable incorporation of common Pb.

A range of LA-ICPMS U-Pb dating applications are presented and include U-Pb dating of apatite from >3.8 Ga gneisses from Akilia, SW Greenland. These apatites host ^{13}C-depleted graphite inclusions that are interpreted as biogenic in origin and representing the oldest indications of life on Earth. The U-Pb age profiles on single apatite grains presented here are characteristic of Pb loss by volume diffusion with core-rim age differences of up to 300 Ma. These data explain the scatter and poor precision of earlier U-Pb apatite age determinations on Akilia apatite. Other LA-ICPMS dating applications include U-Pb apatite dating as a rapid method for determining the age of mafic intrusions, U-Pb titanite and apatite dating of ash fall tuffs, determining temperature-time histories using multiple U-Pb thermochronometers and improving concordance in LA-ICPMS primary zircon standard datasets by analysing young, common Pb-bearing primary zircon standards that have not accumulated significant radiation damage.

1. Introduction

U-Pb dating of accessory minerals has been revolutionised in the last decade by substantial improvements of the LA-ICPMS technique, which offers low-cost, rapid data acquisition compared to the ID-TIMS or ion microprobe U-Pb methods (e.g., Košler and Sylvester, 2003). The high sample throughput afforded by LA-ICPMS has made it a routine tool in sedimentary provenance studies, particularly in U-Pb dating of detrital zircon. Recent analytical developments in mass spectrometer and laser ablation systems (e.g. McFarlane and Luo, 2012) have facilitated progressively smaller spot sizes and shorter analysis times (e.g. Cottle et al., 2012) with a precision approaching that of ion microprobe analysis.

The challenges involved in U-Pb dating of accessory minerals such as zircon by LA-ICPMS include the problem of laser-induced U-Pb downhole fractionation during an analysis, and instrument drift (the change in sensitivity with time) during the course of an analytical

session. The various strategies employed for correcting for downhole U-Pb fractionation are discussed in detail later, but generally involve using an external standard of known age to derive an empirical downhole correction factor that can then be applied to the unknown sample (e.g., Jackson et al. 1996). Instrument drift during an analytical session can also be corrected for using the sample-standard bracketing approach.

For this reason, the LA-ICPMS U/Pb dating method is particularly reliant on high-quality reference materials. These materials must be homogenous in terms of their U/Th/Pb age systematics and free of (or at very least homogenous in terms of) common Pb, such as the zircon standard 91500 (Wiedenbeck et al., 1995). Many other U/Pb age reference materials have been proposed but many suffer to variable extent from issues such as occasional localized discordance, and occasional and variable localized incorporation of common Pb (e.g. SL 13 zircon, Kinny et al., 1991; R33 zircon, Black et al., 2004; Khan titanite, Heaman et al., 2009). Apart from zircon, monazite and baddelyite, many common U- and Th-bearing accessory minerals typically accommodate significant amounts of common (or initial) Pb in their crystal structure (e.g. apatite, titanite, allanite and rutile). As such, these phases often have low U and Pb concentrations and low radiogenic Pb / common Pb ratios which necessitate common-Pb correction. This is either achieved in concordia or isochron plots of a suite of co-genetic grains with a large spread in radiogenic Pb / common Pb ratio or alternatively a Pb-correction is applied to individual analyses based on an appropriate choice of initial Pb isotopic composition. The need to correct for common Pb, U-Pb downhole fractionation and instrument drift makes U-Pb dating of common Pb-bearing accessory minerals challenging.

Although there have been several successful LA-ICPMS U-Pb dating studies (on both single collector and multi-collector instruments) of apatite (e.g. Storey et al., 2007; Chew et al.,

2011; Thomson et al., 2012), titanite (e.g. Kohn and Corrie, 2011; Sun et al., 2012; Spencer et al., 2013) and rutile (e.g. Zack et al., 2011) to date there has been no universal approach to U-Pb dating of common Pb-bearing accessory minerals by LA-ICPMS. The method presented here uses a modified version of the VizualAge U-Pb data reduction package (Petrus & Kamber, 2012) for Iolite (Paton et al., 2011). The chief advantage of the chosen Iolite-based approach is that it can employ any accessory mineral standard, even if it contains significant and *variable* amounts of common Pb, and it can be applied to raw data files exported from the majority of modern ICPMS instruments.

2. Challenges in U-Pb dating of common Pb-bearing accessory minerals

2.1 Downhole U-Pb fractionation

Elemental fractionation is an important consideration in U-Pb dating of accessory minerals by LA-ICPMS. Several strategies have been employed to both minimize this fractionation and to correct for it, primarily in U-Pb dating studies of zircon, and the reader is referred to Košler and Sylvester (2003) for a detailed account of these techniques. Approaches for minimizing U-Pb fractionation include generating a large, shallow laser pit by either spot ablation (Eggins et al. 1998) or by rastering (Košler et al. 2002), to ablate in He instead of Ar, and to use a 2-volume sample cell.

One approach to correct for U-Pb downhole fractionation is that of Košler et al. (2002). Termed the intercept method, it is based on the premise of Sylvester and Ghaderi (1997) that laser-induced, volatile/refractory element fractionation is a linear function of time and can therefore be corrected by extrapolating the measured U-Pb ratios back to the start of ablation. This approach eliminates potential matrix differences between external standards and unknown samples because the measured ratios at the start of ablation are calculated from the

data for each individual sample. This method has been applied U-Pb LA-ICPMS dating of zircon (Košler et al., 2002), monazite (Košler et al., 2001) and apatite (Chew et al., 2011) and is well suited to target minerals for which no well characterised matrix-matched standard exists.

The most commonly used approach to correcting for U-Pb downhole fractionation in LA-ICPMS dating of accessory minerals is to characterise the downhole U-Pb signal response using a matrix-matched standard (e.g., Jackson et al. 1996). A matrix-matched standard is usually required because different accessory minerals (e.g., apatite, titanite and zircon) show different time-resolved U-Pb signals during ablation (e.g., Gregory et al. 2007). Early studies have typically assumed that the pattern of fractionation with hole depth was linear but recent studies (e.g. Paton et al., 2010) have demonstrated that nonlinear, session-specific models of downhole fractionation are more appropriate.

2.2 Instrument drift and instrumental U/Th/Pb fractionation

Although modern LA-ICPMS systems generally yield relatively stable signals for extended periods of time, instrument drift during analytical sessions does occur and has to be corrected for to ensure good quality quantitative analyses. Solution-based measurements by ICPMS generally employ an internal and/or external standardisation where all data are normalised to an isotope present in known concentrations in all samples and standards (e.g. Eggins et al., 1997). A similar strategy is behind the intercept method of Košler et al. (2002) where variations in sensitivity during a U-Pb LA-ICPMS analytical session are corrected for by aspirating a tracer solution (e.g. Tl–U–Bi–Np) with the sample into the plasma. However simultaneous aspiration of a tracer solution to correct for instrument drift results in decreased sensitivity and increased oxide production when compared to “dry” LA-ICPMS analyses. The sample-standard bracketing approach used to correct for U-Pb downhole fractionation is

also the most commonly used method to correct for instrument drift in U-Pb dating by LA-ICPMS, as drift in U-Pb ratios caused by variations in sensitivity during an analytical session can be accounted for by interspersing the unknown samples with matrix-matched external U-Pb age standards.

An important premise of successful U-Pb dating with the matrix-matched sample-standard bracketing method is the lack of even subtle matrix effects. Theoretically, for stoichiometric minerals such as zircon, there should be no significant matrix differences between different grains of zircon. However, because U-bearing minerals have variably radiation damaged lattices, it is possible and indeed likely that the UV-laser beam will interact slightly differently with grains of variable lattice damage. The resulting aerosol may therefore contain particle size distributions that are different from one mineral to the next, even when the matrix is identical in terms of its chemistry. Because Th, U and Pb have different first ionisation potentials, particle size does affect the extent to which these elements are ionised. To minimise the effect of particle size distribution on effective ionisation and hence apparent U/Th and U/Pb ratios, ICP-MS instruments are tuned to yield near-equal response for Th and U. This involves ablation of a glass standard with identical Th and U content and adjustment of torch position (plasma sampling depth) and Ar and He gas flows to yield acceptable sensitivity and a Th/U ratio of between 0.9 and 1.0. The majority of ICPMS instruments, when tuned for maximum sensitivity, will yield Th/U << 0.9 and in this mode of operation, are prone to particle-size induced Th/U/Pb fractionation. In the present study, an ICPMS with a free running, rugged 27.12 MHz solid state RF plasma generator was used which was capable of maintaining a plasma even at unreasonably high (e.g. 3 L min^{-1}) He flows and which could easily be tuned to deliver high sensitivity with Th/U between 0.9 and 1.0 with He flows greater than 1 L min^{-1}.

2.3 Common Pb

U-bearing accessory minerals such as apatite, titanite, allanite and rutile can accommodate a significant amount of initial Pb in their crystal structure and arguably the major limitation on the accuracy and precision of U-Pb dating of these phases is the need to use a common-Pb correction. Common Pb correction typically is undertaken using either concordia or isochron plots on a suite of co-genetic grains or alternatively on individual analyses using an appropriate choice of initial Pb isotopic composition. A brief summary of these approaches is given below as the VizualAge_UcomPbine can employ several different methods to undertake common Pb corrections on both age standards and unknowns. The reader is referred to Ludwig (1998) and Williams (1998) for more information.

Concordia or isochron plots on a suite of co-genetic grains do not require an estimate of the initial Pb isotopic composition but instead require a large spread in radiogenic Pb / common Pb ratios. The Total-U/Pb isochron, a three-dimensional $^{238}U/^{206}Pb$ vs. $^{207}Pb/^{206}Pb$ vs $^{204}Pb/^{206}Pb$ plot (Ludwig, 1998), does not assume concordance and also yields the smallest error of any possible U/Pb or Pb/Pb isochron as all relevant isotope ratios are used at the same time. Other isochrons, such as the $^{238}U/^{204}Pb$ vs $^{206}Pb/^{204}Pb$, $^{235}U/^{204}Pb$ vs $^{207}Pb/^{204}Pb$ and $^{207}Pb/^{204}Pb$ vs $^{206}Pb/^{204}Pb$ plots all assume the U-Pb* data (where Pb* = the radiogenic Pb component) are concordant to calculate accurate isochron dates. Another approach often employed in U-Pb dating of high common Pb phases, such as the LA-ICPMS U-Pb dating studies of titanite (Simonetti et al., 2006) and apatite (Chew et al., 2011) involves projecting a straight line through the uncorrected data on a Tera–Wasserburg Concordia to determine the common Pb-component (y-intercept) on the $^{207}Pb/^{206}Pb$ axis. The $^{238}U/^{206}Pb$ age can then be calculated as either a lower intercept $^{238}U/^{206}Pb$ age on the concordia or as a weighted average of ^{207}Pb-corrected ages using the concordia $^{207}Pb/^{206}Pb$ intercept as an estimate of the

initial Pb isotopic composition. This approach also assumes that the U-Pb* data are concordant and equivalent.

The alternative approach involves correcting individual analyses for initial Pb prior to age calculations. The best estimates of initial Pb isotopic compositions are derived by analysing a low-U co-genetic phase (e.g. feldspar) which exhibits negligible in-growth of radiogenic Pb. If such data are not available initial Pb can be estimated from Pb evolution models (e.g., Stacey and Kramers, 1975; Kramers and Tolstikhin, 1997). The latter approach is the only option for U-Pb dating of detrital accessory minerals containing common Pb. Three separate strategies exist: the ^{204}Pb-, ^{207}Pb- and ^{208}Pb-correction methods (Williams, 1998). The main advantage of the ^{204}Pb correction method is that it does not assume U/Pb* concordance. It does require accurate measurement of ^{204}Pb and is sensitive to the low ^{206}Pb/^{204}Pb ratios encountered in Phanerozoic samples (e.g. Cocherie et al., 2009) and is thus ideally suited to U-Pb dating by high-precision ID-TIMS or MC-ICPMS analyses (e.g. Gehrels et al., 2008; Thomson et al., 2012). However the ability to identify concordance in the ^{204}Pb-corrected data can be obscured by an inappropriate choice of initial Pb. Both the ^{207}Pb- and ^{208}Pb-correction methods assume initial concordance in ^{238}U/^{206}Pb - ^{207}Pb/^{206}Pb and ^{238}U/^{206}Pb - ^{208}Pb/^{232}Th space, respectively. The ^{207}Pb-correction method is widely used in U-Pb ion microprobe studies (Gibson and Ireland, 1996), and only requires precisely measured ^{238}U/^{206}Pb and ^{207}Pb/^{206}Pb ratios and an appropriate choice of common Pb. The ^{208}Pb-correction method is less commonly applied. It requires the measurement of ^{208}Pb/^{206}Pb and ^{232}Th/^{238}U and an appropriate choice of initial ^{208}Pb/^{206}Pb, and works well for samples with low Th/U (e.g., < 0.5) (Cocherie, 2009; Williams 1998). A variant on the ^{208}Pb-correction method is applied in U-Pb dating studies of rutile. The Th contents of granulite-facies rutile are often extremely low, meaning that all ^{208}Pb measured can be attributed to common Pb, yielding a much more accurate common Pb correction than can be obtained using the ^{204}Pb

method (e.g. Zack et al., 2011). To avoid confusion, this variant of the ^{208}Pb-based common Pb correction is referred to in this study as the $^{208}Pb_{(no\ Th)}$ method.

2.4 Suitable matrix-matched standards

Until relatively recently U-Pb dating of common Pb-bearing accessory minerals by LA-ICPMS dating (particularly apatite) has been hindered by the lack of well-characterized matrix-matched reference materials to correct for elemental fractionation.

The LA-MC-ICPMS U-Pb apatite dating study of Thomson et al. (2012) characterised two natural reference apatite samples: blue/green gem apatite roughs from the "1st Mine Discovery", Madagascar, and apatite from the McClure Mountain syenite, Colorado (Schoene and Bowring, 2006). Thomson et al. (2012) dated two gem quality c. 1 cm sized crystals of Madagascar apatite by U-Pb ID-TIMS, obtaining weighted average ^{206}Pb-^{238}U ages of 485.0 ± 1.7 and 474.2 ± 0.4 Ma respectively. Although these smaller shards differ in age by c. 11 Ma (and hence independent ID-TIMS U-Pb characterization must be performed on each crystal fragment), they show excellent internal consistency in their ID-TIMS U-Pb ages and $^{206}Pb/^{204}Pb$ ratios.

A c. 1 cm sized crystal of Madagascar apatite which has yielded a weighted average ID-TIMS concordia age of 473.5 ± 0.7 Ma (Cochrane et al., submitted) was used as the primary apatite reference material in this study. McClure Mountain syenite apatite (the rock from which the $^{40}Ar/^{39}Ar$ hornblende standard MMhb is derived) was used as a secondary standard. McClure Mountain syenite has moderate but reasonably consistent U and Th contents (~ 23 ppm and 71 ppm, Chew and Donelick, 2012) and its thermal history, crystallization age (weighted mean $^{207}Pb/^{235}U$ age of 523.51 ± 2.09 Ma) and initial Pb

isotopic composition ($^{206}Pb/^{204}Pb = 17.54 \pm 0.24$; $^{207}Pb/^{204}Pb = 15.47 \pm 0.04$) are known from high-precision TIMS analyses (Schoene and Bowring, 2006).

Durango apatite and Fish Canyon Tuff apatite were also analysed in this study as secondary standards. Durango apatite is a distinctive yellow-green fluorapatite widely used as a mineral standard in apatite fission-track and (U–Th)/He dating and apatite electron micro-probe analyses. It is found as large crystals within an open pit iron mine at Cerro de Mercado, Durango, Mexico. The apatite formed between the eruptions of two major ignimbrites which have yielded a sanidine-anorthoclase $^{40}Ar–^{39}Ar$ age of 31.44 ± 0.18 Ma (McDowell et al., 2005). The Fish Canyon Tuff is a vast ash-flow sheet (~5000 km^3) of uniform phenocryst-rich dacite from SW Colorado. Sanidine from the Fish Canyon Tuff is widely used as a flux monitor in $^{40}Ar–^{39}Ar$ dating and has yielded an astronomically calibrated age of 28.201 ± 0.046 Ma (Kuiper et al. 2008).

The primary titanite standard analysed in this study is OLT1 titanite which has yielded a TIMS concordia age of 1014.8 ± 2.0 (Kennedy et al., 2010). OLT1 titanite is a large single red-brown crystal sampled from a metasomatic calcite skarn of the Grenville Province of the Canadian Shield. It does exhibit minor ID-TIMS U-Pb age heterogeneity but this heterogeneity is less than that of Khan titanite, which along with Fish Canyon Tuff titanite was employed as a secondary standard in this study. Khan titanite is taken from a pegmatite in the Khan copper mine, Namibia that contains abundant large (cm-size) titanite crystals. It has a relatively uniform chemical composition (U=584 ± 95 ppm; Th=473 ± 73 ppm; Pb=57 ± 8 ppm; Th/U=0.81 ± 0.05). Nine Khan titanite analyses have yielded an ID-TIMS U-Pb upper intercept concordia age of 522.2 ± 2.2 Ma (Heaman et al., 2009), with younger U-Pb ages attributed to sub-domains of crystals which have undergone Pb loss.

The primary rutile standard analysed in this study is R10 rutile from Gjerstad in South Norway. It is a fragment of a large (centimeter-scale) single crystal that has yielded a U–Pb TIMS age of c. 1090 Ma (Luvizotto et al., 2009). The secondary rutile standard R19b is a large (c. 500 mm^3) sized single crystal from Blumberg, Australia that has been studied in detail for a range of trace elements and Hf isotopes (Luvizotto et al. 2009). It has yielded a weighted mean TIMS $^{206}Pb/^{238}U$ age of 489.5 ± 0.9 Ma (Zack et al., 2011).

3. The Iolite approach to LA-ICPMS data reduction

Iolite (http://www.iolite.org.au) (e.g., Hellstrom et al. 2008, Woodhead et al. 2008, Paton et al. 2011) is a software package developed for mass spectrometric data reduction. It was developed as a set of procedures for Igor Pro (http://www.wavemetrics.com), a relatively inexpensive platform for scientific graphing, data analysis and image processing of time series data. Igor Pro comes with its own programming language and can be used in either a Mac or Windows environment. Iolite is capable of processing very large datasets (e.g. multi-hour sessions of laser ablation data) with a strong emphasis on viewing and editing data in graphical form as plots of signal intensity, isotopic ratios or elemental ratios versus time. Iolite itself is provided free of charge and is therefore easily accessible to any laboratory or person wishing to quickly and thoroughly analyse ICP-MS data.

A brief summary of the Iolite approach to mass spectrometric data reduction is outlined here. The data import capabilities of Iolite are one of its many strengths as it can accept raw data files from the vast majority of modern TIMS and ICPMS instruments. Once data have been imported, they are represented inside the software as a time series called a “wave” (Igor Pro terminology) or a “channel” (Iolite terminology) for each of the masses determined. Each data point of a channel corresponds to a single measurement for that channel’s mass at a given sampling time. Segments of data to be used in the data reduction calculations (e.g.

individual analyses of a reference material or an unknown) are defined by the user using the graphical user interface of Iolite and are termed ‘‘integrations”. Defining the integrations visually provides real-time feedback on statistics regarding the integration area. Data reduction of the input channels is undertaken by one of many plug-ins (referred to as a "Data Reduction Scheme" or "DRS") each of which is stored in a discrete, user-editable file. There is a growing number of DRSs that are either supplied with Iolite or are produced by independent developers. This range of DRSs enables Iolite to undertake diverse functions such as baseline subtraction, correcting for instrumental drift, interpolating mass bias, calculating semi-quantitative trace-element abundances or downhole elemental fractionation in U-Pb geochronology.

A typical U-Pb geochronology data reduction session in Iolite using either the built-in U-Pb Geochronology DRS of Paton et al. (2010) or the VizualAge DRS of Petrus and Kamber (2012) starts with the user defining baseline integrations to generate session-wide baseline-corrected values for each isotope. The user then defines integrations for U-Pb reference materials (e.g. 91500 zircon) and unknowns. Both the U-Pb Geochronology DRS and the VizualAge DRS characterise the time-resolved fractionation response of individual standard analyses using a user-specified downhole correction model (such as an exponential curve, a linear fit or a smoothed cubic spline). The advantage of this approach is that it has the versatility to treat data from any laboratory, regardless of the expression of the downhole fractionation. The DRS then fits this appropriate session-wide “model” U-Th-Pb fractionation curve to the time-resolved standard data and the unknowns. Sample-standard bracketing is applied after the correction of downhole fractionation to account for long-term drift in isotopic or elemental ratios by normalizing all ratios to those of the U-Pb reference standards. As with baseline subtraction, Iolite has the option of using a variety of user-specified splines to interpolate normalization factors from the reference standard analyses through unknowns.

The output channels are then populated with the final isotopic and elemental ratios and ages used in U-Pb geochronology studies.

3.1 VizualAge and the new common Pb data reduction scheme

The VizualAge DRS (Petrus and Kamber, 2012) is a set of Igor Pro procedures that work with Iolite to provide advanced U-Pb geochronology data reduction and visualisation capabilities. It expands upon the original Iolite U-Pb geochronology DRS (Paton et al. 2010) by calculating $^{207}Pb/^{206}Pb$ ages and common Pb corrections for each time-slice of raw data, along with live concordia diagrams for visualising of data while adjusting integration intervals. These live diagrams include conventional (Wetherill), inverse (Tera-Wasserburg), 3D U-Th-Pb and total U-Pb concordias and provide instantaneous feedback regarding discordance, uncertainty, error correlation and common Pb. The original VizualAge DRS can undertake common Pb corrections on unknowns using an initial Pb isotope composition calculated using the Stacey & Kramers (1975) terrestrial Pb evolution model for the crystallization age of the accessory mineral in question. However both it and the U-Pb geochronology DRS of Paton et al. (2010) assume that the U-Pb reference standards are free of common Pb. However, all the U-Pb apatite and titanite reference materials investigated in this study contain appreciable (and usually variable) amounts of common Pb, and hence a common Pb correction needs to be applied to the reference materials prior to corrections for downhole fractionation and instrument drift. More details on the how the common Pb-correction is applied to the standards is given in the Appendix.

The data reduction scheme presented here (VizualAge_UcomPbine) undertakes a common Pb correction using either the ^{204}Pb, ^{207}Pb or $^{208}Pb_{(no\ Th)}$ methods for the initial Pb isotope composition(s) specified in the accompanying standard reference values file. The effect of the common Pb correction on reference standard data with appreciable and variable common Pb

is illustrated in Fig. 1. In this example (analyses of McClure Mountain apatite) a model downhole $^{207}Pb/^{235}U$ fractionation curve was fitted without a common Pb correction (Fig. 1a) and with a ^{207}Pb-based common Pb correction (Fig. 1b) using an initial $^{207}Pb/^{206}Pb$ value of 0.88198 derived from an apatite ID-TIMS total U-Pb isochron (Schoene and Bowring, 2006). McClure Mountain apatite is a multi-grain mineral separate from a syenite and the crystals show substantial inter-crystal variability in their $^{207}Pb/^{235}U$ and $^{206}Pb/^{238}U$ ratios, with raw $^{207}Pb/^{235}U$ ratios ranging from c. 1 - 4.5 (Fig. 1a). The remaining difference between the model $^{207}Pb/^{235}U$ fractionation curve and the accepted radiogenic $^{207}Pb/^{235}U$ ratio of 0.6746 (Schoene and Bowring, 2006) after the common Pb correction has been applied (Fig. 1b) is attributed to the mass discrimination from ablation to detector. Session-wide (i.e. long term) drift in the mass discrimination is subsequently accounted for by sample-standard bracketing.

In this study a ^{207}Pb-based common Pb correction was applied to most of the U-Pb reference materials (Fig. 2) as precise measurements of the low intensity ^{204}Pb peak with single-collector instruments require a prohibitively long dwell time and there is the additional complication of the isobaric mass-204 interference caused by ^{204}Hg in the gas supply. The ^{207}Pb correction assumes that the sample U-Pb* data (where Pb* = the radiogenic Pb component) are concordant. In the case of U-Pb reference materials, the supposition of concordance were no initial Pb present is a reasonable assumption. The DRS was also tested using the ^{204}Pb- and $^{208}Pb_{(no\ Th)}$-based corrections on standards (Fig. 2E, 2F). A ^{204}Pb-based correction is appropriate for multi-collector instruments which can measure ^{204}Pb precisely (isobarically corrected for ^{204}Hg), while a $^{208}Pb_{(no\ Th)}$-based correction is ideally suited for U-Pb dating of accessory minerals (typically rutile) which have negligible Th contents meaning that all the measured ^{208}Pb can be attributed to common Pb (e.g. Zack et al., 2011).

Following common Pb correction of the standard reference materials, a session-wide drift correction is undertaken by sample-standard bracketing. The final isotopic and elemental ratios and age channels of the original VizualAge DRS are now augmented in the new DRS by ^{207}Pb-corrected and $^{208}Pb_{(no\ Th)}$-corrected age channels (calculated for user-specified initial Pb ratios for a given integration type) so the U-Pb ages of unknowns can be monitored in Iolite. The ^{204}Pb-based common Pb correction of the original VizualAge DRS (Petrus and Kamber, 2012) is also available, and this too can accommodate user-specified initial Pb ratios. All other conventional common Pb correction methods (e.g. intercept ages calculated from linear arrays on a concordia or isochron) can be performed offline. Common-Pb corrected U-Pb ages of all integrations (both standards and unknowns) can also be monitored on conventional (Wetherill) and inverse (Tera-Wasserburg) concordia diagrams using the ^{204}Pb- and $^{208}Pb_{(no\ Th)}$-based common Pb correction methods.

The most recent version of VizualAge can be obtained from http://www.japetrus.net/va. Following installation of VizualAge, the additional files required for the VizualAge_UcomPbine DRS can be found at http://www.japetrus.net/va/UcomPbine/

4. Results: standard data

The VizualAge_UcomPbine DRS was tested on the apatite and titanite age standards listed in section 2.4 using a Photon Machines Analyte Excite 193 nm ArF Excimer laser ablation system coupled to a Thermo Scientific iCAP-Qc (Q-ICP-MS) at the Department of Geology, Trinity College Dublin. The DRS was also employed on a common Pb-bearing primary zircon standard (section 5.6) using a Resonetics RESOlution M-50 193 nm ArF excimer laser ablation system coupled to a Thermo X Series II Q-ICP-MS at the Department of Earth Sciences, Laurentian University. The analytical parameters for both setups are listed in Table 1 and are summarized here.

With the exception of the U-Pb apatite sample where a suite of trace and rare earth elements were also analysed (Table 1, Fig. 3E), most analysis cycles employed only the elements typically used in U-Th-Pb geochronology (^{238}U, ^{232}Th, ^{204,206,207,208}Pb), one or two isotopes of Hg (^{200,202}Hg) and an internal elemental standard (^{43}Ca for apatite and titanite, ^{49}Ti for rutile and ^{91}Zr for zircon). In addition to providing a means by which to normalize concentration data, the time-resolved signal intensity of the internal elemental standard is often used in Iolite to define the start and end of an ablation ("beam seconds" in Iolite terminology). The dwell times for individual isotopes were adjusted to yield similar total counts per isotope in each analysis cycle. However following this strategy for ^{204}Pb would result in a prohibitively long dwell time for this isotope, and so for those samples that employed the ^{207}Pb-based correction, a dwell time corresponding to a maximum of 20% of the total analysis cycle was used. A longer baseline (50 s as opposed to 15 s), a longer dwell time on ^{204}Pb (30% of the total analysis cycle) and a large spot size (130 μm) were employed to yield a sufficiently large and precise baseline-corrected ^{204}Pb signal to the test the ^{204}Pb correction on Durango apatite in Fig. 2E.

All analytical data are listed (287 apatite and titanite U-Pb analyses, 29 rutile analyses and 48 zircon U-Pb analyses) in the supplementary data table (Table SD1). All apatite, titanite and rutile ages and U, Th and Pb concentration data (obtained by normalising the apatite, titanite and rutile background-corrected signals relative to NIST 612 standard glass and using ^{43}Ca or ^{49}Ti as an internal standard) are summarised in Table 2.

4.1 Apatite standard data

A c. 1 cm crystal of Madagascar apatite was used as the primary apatite reference material in this study. Fragments of this crystal have yielded a weighted average ID-TIMS concordia age of 473.5 ± 0.7 Ma corrected using a ^{204}Pb common Pb-correction with an initial ^{207}Pb/^{206}Pb

value of 0.8681 derived from the Stacey & Kramers (1975) terrestrial Pb evolution model (Cochrane et al., submitted). A ^{207}Pb correction was applied to the primary standard in Figs 2A and 2B and a ^{204}Pb correction was applied to the primary standard in Fig. 2E.

Thirty-three analyses of McClure Mountain apatite (^{207}Pb/^{235}U TIMS age of 523.51 ± 1.47 Ma; Schoene & Bowring, 2006) yielded a U-Pb Tera-Wasserburg concordia lower intercept age of 524.5 ± 3.7 Ma (Fig 2A) with an MSWD = 0.72. The lower intercept was anchored using a ^{207}Pb/^{206}Pb value of value of 0.88198 derived from an apatite ID-TIMS total U-Pb isochron (Schoene and Bowring, 2006). The age obtained in this study is accurate within the ID-TIMS error. The same sample yields an inaccurate ^{206}Pb/^{204}Pb vs ^{238}U/^{204}Pb isochron of 464±35 Ma (MSWD = 1.5) anchored using the initial ^{206}Pb/^{204}Pb estimate of 17.49±0.26 of Schoene & Bowring (2006), demonstrating the difficulty in measuring precisely the low intensity ^{204}Pb peak on a single-collector instrument when the analytical setup is not optimised for a ^{204}Pb-based correction.

Thirty-six analyses of Durango apatite (31.44 ± 0.18 Ma; McDowell et al., 2005) yielded a U-Pb Tera-Wasserburg concordia lower intercept age of 31.97 ± 0.59 Ma (Fig. 2B) with an MSWD of 1.07. The lower intercept was anchored using a ^{207}Pb/^{206}Pb value of 0.8376 derived from the Stacey & Kramers (1975) terrestrial Pb evolution model. Anchoring the U-Pb Tera-Wasserburg concordia with a ^{207}Pb/^{206}Pb value of 0.8244 derived from the Kramers and Tolstikhin (1997) Pb evolution model yields a lower intercept age of 31.82 ± 0.59 Ma (Fig. 2B) with an MSWD of 1.06. Using the analytical setup optimised for a ^{204}Pb-based correction (50 s baseline, longer dwell time on ^{204}Pb, 130 μm spot size, Table 1) and initial Pb isotopic ratios derived from the Stacey & Kramers (1975) terrestrial Pb evolution model, thirty-one analyses of Durango apatite yielded a U-Pb concordia lower intercept age of 31.86 ± 0.46 Ma (Fig. 2E) with an MSWD of 0.46. Applying a ^{204}Pb-correction to these analyses

yielded a concordia age of 31.82 ± 0.40 Ma (Fig. 2E) with an MSWD of 1.4, demonstrating the suitability of the ^{204}Pb-correction. All the Durango ages obtained in this study are accurate within the analytical uncertainty of the McDowell et al. (2005) age.

4.2 Titanite standard data

The primary titanite standard analysed in this study is OLT1, which has yielded a TIMS concordia age of 1014.8 ± 2.0 (Kennedy et al., 2010). The primary standard was corrected using a ^{207}Pb-based correction. Twenty analyses of Fish Canyon Tuff titanite (astronomically calibrated age of 28.201 ± 0.046 Ma, Kuiper et al. 2008) yielded a U-Pb Tera-Wasserburg concordia lower intercept age of 28.78 ± 0.41 Ma (Fig 2C) with an MSWD = 1.41. The lower intercept was anchored using a ^{207}Pb/^{206}Pb value of 0.8444 derived from TIMS Pb isotopic measurements of Fish Canyon Tuff sanidine (Hemming and Rasbury, 2000). The age obtained in this study is 0.58 Ma older than the astronomically tuned age, somewhat outside the analytical error of 0.41 Ma.

Fourteen analyses of Khan titanite (522.2 ± 2.2 Ma, Heaman et al., 2009) yielded a U-Pb Tera-Wasserburg concordia lower intercept age of 520.9 ± 3.9 Ma (Fig. 2D) with an MSWD of 4.2. The lower intercept was anchored using a ^{207}Pb/^{206}Pb value of 0.8714 derived from the Stacey & Kramers (1975) terrestrial Pb evolution model. This age is accurate within the uncertainty of the ID-TIMS datum.

4.3 Rutile data

The primary standard analysed in this study is the R10 rutile that has yielded a U–Pb TIMS age of c. 1090 Ma (Luvizotto et al., 2009). The primary standard was corrected using a ^{208}Pb$_{(no\ Th)}$-based correction although the majority of R10 rutile analyses are concordant without common Pb correction. Twenty-nine analyses of a large (> 1cm^2) rutile from a

Caledonian quartz vein from the Dalradian Supergroup of the Grampian Highlands of Scotland were undertaken to test the $^{208}Pb_{(no\ Th)}$-based common Pb correction. The data uncorrected for common Pb yield a U-Pb TW concordia intercept age of 452.6 ± 4.7 Ma (MSWD = 0.89), with variable incorporation of common Pb (Fig. 2F). The $^{208}Pb_{(no\ Th)}$-corrected data are concordant on TW Concordia, and yield a concordia age of 448.6 ± 4.5 Ma (MSWD = 1.4) demonstrating the suitability of the $^{208}Pb_{(no\ Th)}$-based common Pb correction.

5. Applications

The standard data demonstrate the accuracy and precision that can be attained with Excimer laser ablation systems coupled to latest generation Q-ICPMS instruments, with 2σ uncertainties of <1% on Phanerozoic apatite and titanite standards and 2σ uncertainties of <2% on Paleogene apatite and titanite standards. In this section applications of U-Pb dating of common Pb-bearing accessory minerals by LA-ICPMS are presented. Unlike the standards, which are selected for favourable U/Pb ratios, many of the samples in this section are challenging to date as they have low U contents and / or little radiogenic Pb and /or high common Pb. All of these data were produced using the analytical setup described previously and were reduced using the VizualAge_UcomPbine DRS. The analytical parameters are listed in Table 1, while all data are listed in the supplementary data table (Table SD1) and are summarised in Table 2. All primary standards in this section were corrected using a ^{207}Pb-based correction. These applications include obtaining U-Pb crystallisation ages from basic intrusive rocks, U-Pb dating of ash-fall tuffs, producing temperature-time histories using multiple U-Pb thermochronometers and U-Pb dating of Akilia Island apatite which hosts graphite inclusions previously interpreted as representing the oldest indications of life on Earth. Strategies for optimising the spread in radiogenic Pb / common Pb ratios on a concordia diagram and for improving concordance in LA-ICPMS primary zircon standard

datasets by analysing young, common Pb-bearing primary zircon standards are also presented.

5.1 U-Pb dating of apatite-bearing basic intrusives

Obtaining crystallisation ages from basic plutonic rocks can be challenging, and is usually undertaken by U-Pb zircon or baddelyite dating or ^{40}Ar-^{39}Ar dating of fresh magmatic plagioclase. However zircon is not particularly common in silica-poor magmas (Hoskin and Schaltegger 2003), baddelyite is difficult to separate, and plagioclase is susceptible to alteration, particularly in oceanic environments. Additionally, the low K contents of plagioclase mean that the incorporation of excess argon can have a large effect on measured ^{40}Ar-^{39}Ar ages (McDougall and Harrison, 1999). By contrast, apatite is a common phenocryst phase in many gabbros and dolerites (Piccoli and Candela, 2002) and is easily separated from other minerals and U-Pb LA-ICPMS apatite dating thus offers a rapid and convenient alternative to dating basic intrusive rocks.

The sample dated in Fig. 3A is a dolerite sill of hitherto unknown age which cuts Mississippian limestones at Ballinalack, Ireland. The principal phenocrysts are plagioclase, clinopyroxene and minor olivine. Apatite was not observed in thin section but is present as a minor accessory phase in the non-magnetic heavy fraction ($\rho > 2.9$ g cm^{-3}). Forty spot analyses yielded a U-Pb Tera-Wasserburg concordia lower intercept age of 58.9 ± 3.5 Ma (Fig. 3B) with an MSWD of 1.4. This age confirms that the dolerite belongs to the main phase of volcanism (61 – 59 Ma; Chambers et al., 2001) of the British – Irish Palaeogene Igneous Province, associated with the proto-Iceland plume. The date is reasonably precise (± 3.5 Ma) considering the young age of the sample and the low U content of the apatite (~ 5 ppm, Table 2).

5.2 U-Pb dating of common Pb-bearing phenocrysts in ash-fall tuffs

Many ash fall-tuffs contain apatite and / or titanite as phenocrysts, and U-Pb dating of these phases is useful in cases where magmatic zircon is either not present or exhibits marked inheritance or Pb loss. In Fig. 3B, U-Pb apatite data from the lower Eifelian Tioga Ash Bed (Old Port, Pennsylvania, U.S.A.) are presented. In the apatite phenocrysts of this sample, the advantage of relatively high U contents (33.4 ppm, Table 2) is offset by significant common Pb. Eighteen spot analyses yielded a U-Pb Tera-Wasserburg concordia lower intercept age of 392.1 ± 5.1 Ma (Fig. 3B) with an MSWD of 0.92. This age is in good agreement with the U-Pb TIMS monazite age of 390.0 ± 0.5 Ma of Roden et al. (1990), and the U–Pb TIMS zircon age of 391.4 ± 1.8 Ma (Tucker et al., 1998) from the same ash layer.

The initial $^{207}Pb/^{206}Pb$ ratio of the Fish Canyon Tuff titanite sample (Fig. 2C) was constrained by TIMS Pb isotopic measurements of co-magmatic sanidine (Hemming and Rasbury, 2000). In Fig. 3D, U-Pb apatite and titanite data from the Fish Canyon Tuff are presented on a Tera-Wasserburg concordia diagram. In this example, the lower intercept age is not anchored through an initial $^{207}Pb/^{206}Pb$ ratio but rather avails of the large spread in radiogenic Pb ratios between the apatite and titanite analyses to constrain the isochron. Thirty-seven apatite and titanite analyses yield a U-Pb Tera-Wasserburg concordia lower intercept age of 29.14 ± 0.7 Ma (Fig. 3C) with an MSWD of 1.7 which is marginally outside of analytical uncertainty of the astronomically calibrated age of 28.201 ± 0.046 Ma for Fish Canyon Tuff sanidine (Kuiper et al. 2008).

5.3 U-Pb thermochronology of common-Pb bearing accessory minerals

U-Pb dating of apatite and titanite is employed in high-temperature thermochronology studies, with empirical and experimental closure temperatures of ca. 425–550°C calculated

for apatite (Chamberlain & Bowring 2000, Schoene & Bowring 2007, Cherniak et al., 1991). Experimental closure temperatures of titanite (500–650°C, Cherniak, 1993) diverge from empirical closure temperatures estimates derived from geological case studies which range from 650–700°C (Scott and St-Onge, 1996) to significantly higher temperatures (Spencer et al., 2013).

The samples selected as a thermochronology case study in Figs. 3D and 3E are a metabasite (DC 4/5/1) and a granodiorite (DC 4/5/2) from the Eastern Cordillera of Peru (Chew et al., 2007). The metabasite was emplaced as a dyke within the granodiorite and both units share the same pervasive high-grade foliation. The crystallization of the granodioritic protolith has been constrained by a U-Pb TIMS zircon concordia age of 442.4 ± 1.4 Ma and a LA-ICPMS U-Pb zircon concordia age of 444.2 ± 6.4 Ma (Chew et al., 2007). The granodiorite exhibits conspicuous augen of relic igneous plagioclase along with a metamorphic assemblage of garnet, biotite, muscovite, epidote and plagioclase. Thermobarometric estimates for the peak metamorphic conditions are 700 ˚C and 12 kbar (Chew et al., 2005). Both samples contain accessory titanite and apatite.

The titanite data from both samples are plotted on a Tera-Wasserburg concordia diagram (Fig. 3D). The lower intercept age is unanchored but is well constrained due to the large spread in radiogenic Pb / common Pb ratios between the titanite from the metabasite (sample DC 4/5/1) and the granodiorite (sample DC 4/5/2). Thirty-two titanite analyses yield a U-Pb Tera-Wasserburg concordia lower intercept age of 437.1 ± 5.3 Ma (Fig. 3D) with an MSWD of 4.4. Unlike the majority of the LA-ICPMS analyses in this study, the apatite data from sample DC 4/5/2 were acquired using a 30 μm spot size (Table 1). These analyses formed part of an earlier LA-ICPMS study, integrating apatite fission track and U–Pb dating (Chew and Donelick, 2012). This study combined trace element and U-Th-Pb isotopic analyses,

including the absolute U concentration measurements required for fission-track dating. Seventeen apatite analyses from sample DC 4/5/2 yielded a U-Pb Tera-Wasserburg concordia lower intercept age of 365 ± 14 Ma (Fig. 3E) with an MSWD of 2.1. The intercept was anchored using an initial $^{207}Pb/^{206}Pb$ value of 0.857 ± 0.008 derived from LA-MC-ICPMS Pb isotopic analyses of K-feldspar (Chew et al., 2011). The apatite data from sample DC 4/5/1 are not presented on Fig. 3E. They have extremely low U contents (around 1 ppm), and nine apatite analyses with the lowest $^{238}U/^{206}Pb$ ratios (<0.2) yield an average $^{207}Pb/^{206}Pb$ value of 0.8564 ± 0.027. This value is nearly identical to the initial $^{207}Pb/^{206}Pb$ value determined for sample DC 4/5/2, demonstrating that the granodiorite and metabasite were in Pb isotopic equilibrium at their time of formation.

The LA-ICPMS U-Pb zircon, titanite and apatite ages and an unpublished fission track age of 9.1 ± 2.8 Ma (where the U concentration measurements were also acquired by LA-ICPMS) for sample DC 4/5/2 are plotted against estimates of their respective closure temperatures on a temperature-time history diagram (Fig. 3F). The U-Pb zircon age is interpreted as dating the formation of the granitic protolith at 444.2 Ma, with the titanite age of 437.1 Ma ± 5.3 Ma recording either peak metamorphism or rapid cooling from the metamorphic peak at 700 ˚C, 12 kbar. The U-Pb apatite age of 365 Ma ± 14 Ma records subsequent slow cooling through the apatite closure temperature of c. 450 ˚C. The apatite fission track age is interpreted as recording rapid exhumation through the apatite fission track partial annealing zone (60 – 120 ˚C) at 9.1 ± 2.8 Ma which is related to a phase of Late Neogene Andean uplift in the Eastern Cordillera of Peru.

5.4 U-Pb dating of Akilia Island apatite

Mojzsis et al. (1996) reported the presence of ^{13}C-depleted graphite inclusions in apatite from an early Archaean quartz–amphibole–pyroxene (qtz-am-px) gneiss on the island of Akilia,

SW Greenland. The graphite inclusions were interpreted as biogenic in origin and proposed to represent the oldest indications of life on Earth. The gneissic protolith was interpreted as banded iron formation (BIF) and interlayered within mafic gneisses of presumed volcanic origin. These mafic gneisses are in turn inferred to be cut by >3.85 Ga tonalitic gneisses (Nutman et al., 1997). The Akilia discovery has proved highly controversial, with various authors questioning the field relationships and sedimentary origin of the qtz-am-px gneiss (Myers and Crowley, 2000; Whitehouse and Fedo, 2003), the geochronological interpretations (Whitehouse and Kamber, 2005) and even the presence of the graphite inclusions in the apatite (Lepland et al., 2005).

Notwithstanding the controversy, apatite in banded iron formation is potentially a useful capsule for early life biosignatures and can potentially be dated directly, obviating the relevance of controversial field relationships. In the case of the Akilia Island, Sano et al. (1999) and Whitehouse et al. (2009) have presented U-Pb ion microprobe ages for apatite from the Fe-rich gneiss. Sano et al. (1999) reported a $^{238}U/^{204}Pb$ vs $^{206}Pb/^{204}Pb$ isochron of 1504 ± 336 Ma for eleven spot analyses on seven apatite grains. These analyses were undertaken *in situ*, on a polished sample chip of the Fe-rich gneiss, where apatite grains of about 20 – 30 μm diameter were found. The later study by Whitehouse et al. (2009) reported a $^{238}U/^{204}Pb$ vs $^{206}Pb/^{204}Pb$ apatite isochron of 1756 ± 150 Ma. The apatites dated in that study were separated from the original rock from which the graphite inclusions were documented (sample G91-26). The grains were found to have short and long dimensions of 40 - 120 and 60 - 220 μm, respectively. Apatite from sample G91-26 was dated by LA-ICPMS in this study to improve upon the precision of the earlier U-Pb age dating studies.

In contrast to the earlier studies, the apatite analyses for this project were acquired as U-Pb age profiles along c-axis perpendicular apatite surfaces using a 24 μm spot (Table 1) similar

to the methodology of Cochrane et al. (submitted). Two separate age profiles were obtained on grains with a short-axis diameter of 150 μm (grain B) and 330 μm (grain C), respectively (Fig. 3G). The smaller grain (grain B) yields a weighted average ^{207}Pb-corrected age of 1797 ± 24 Ma with no discernible age variation from core to rim while the larger grain (grain C) shows a pronounced age variation with ^{207}Pb-corrected ages as old as 2022 Ma in the core of the grain and as young as 1715 Ma on the rim of the apatite. The age profile for grain C is characteristic of a sample that has undergone thermally activated diffusive loss of a radiogenic isotope during slow exhumation through its respective closure temperature window. Similar Fickian diffusion profiles have been documented for Pb in apatite (Cochrane et al., submitted) and for Ar in muscovite and biotite (e.g. Hodges et al., 1994). Thermally activated volume diffusion of Pb can explain the clear correlation between apatite grain size and U-Pb age. The youngest apatite ages from Akilia are from the study of Sano et al. (1999) which reported ^{238}U/^{204}Pb vs ^{206}Pb/^{204}Pb and ^{207}Pb*/^{206}Pb* isochron ages of c. 1500 Ma on very small apatite grains about 20 - 30 μm in diameter, while this study has recorded apatite ages as old as 2150 Ma in the cores of apatite grains > 300 μm in diameter (Grain A, Table SD1). The scatter and poor precision of the earlier U-Pb age determinations of Akilia Island apatite can be attributed to combining spot analyses from multiple grains of variable size and hence variable closure ages (mixtures of analyses of variable grain size and / or variable positions within individual grains).

5.5 Strategies for optimizing the spread in radiogenic Pb / common Pb ratios

The Tera-Wasserburg concordia diagrams in Figs. 3A-3E illustrate several approaches for constraining the lower intercept age. These approaches include i) using a ^{207}Pb/^{206}Pb initial value calculated using a terrestrial Pb evolution model (Figs. 3A, 3B); ii) using two separate co-magmatic phases from the same rock sample to improve the spread in radiogenic Pb /

common Pb ratios (e.g. the apatite – titanite lower-intercept age for Fish Canyon Tuff in Fig. 3C and the apatite – K-feldspar lower-intercept age for sample DC 4/5/2 in Fig. 3E); and iii) improving the spread in radiogenic Pb / common Pb ratios by analysing the same phase from two rock types of different composition (e.g. the titanite lower-intercept age constructed from a metabasite and granodiorite in Fig. 3D). It is noted that combining data from several radiogenic minerals from one rock can only be done in certain circumstances, most notably for magmatic rocks that cooled reasonably quickly, while combining data from radiogenic minerals from different rocks is only possible in cases where these are consanguineous and share the same initial common Pb composition.

5.6 U-Pb zircon dating using young common Pb-bearing zircon standards

Typically primary LA-ICPMS zircon standards are Palaeozoic or older in age (e.g. 91500 zircon, Wiedenbeck et al., 1995; Plešovice zircon, Slama et al., 2008; Temora zircon, Black et al., 2004) and have moderate to high U concentrations. The rationale is that such standards will yield sufficiently large ^{206}Pb and ^{207}Pb signals for typical laser spot sizes and repetition rates that high precision U/Pb and Pb/Pb ratios can be determined. However using old and / or U-rich primary zircon standards means that portions of the standard crystal lattice are more likely to have experienced radiation damage from natural alpha, alpha recoil, and spontaneous fission processes. It has long been recognised that such radiation-damaged sub-domains are more susceptible to Pb loss (e.g. Krogh and Davis, 1974, 1975) and in U-Pb TIMS dating studies these altered zircon domains are now routinely removed by pre-treating the grains using the chemical abrasion method of Mattinson et al. (2005).

One possibility to improve concordance in LA-ICPMS primary zircon standard datasets would be analyse young primary zircon standards that have not accumulated significant radiation damage. However the low radiogenic ^{207}Pb contents of such zircons typically result

in $^{207}Pb/^{235}U$ ages that are highly imprecise and are also susceptible to yielding erroneously older ages due to incorporation of even minor amounts of common Pb. Figure 4A illustrates a LA-ICPMS zircon dataset where 91500 zircon was used as the primary standard ($^{206}Pb/^{238}U$ TIMS age of 1065.4 ± 0.6 Ma; Wiedenbeck et al., 1995) and Penglai megacryst zircon (SIMS and TIMS $^{206}Pb/^{238}U$ age of 4.4 ± 0.1 Ma; Li et al., 2010) was analysed as an unknown, yielding a Tera-Wasserburg lower intercept age of 4.2 ± 0.12 Ma. Penglai zircon contains substantial amounts of common Pb ($^{207}Pb/^{206}Pb$ ratios as high as 0.8; Fig. 4A), and Li et al. (2010) considered that its young age and high common Pb content made it unsuitable as a primary U–Pb age reference material for LA-ICPMS or SIMS studies. However the precision on the Tera-Wasserburg lower intercept age (Fig. 4A) suggests that Penglai zircon could make a potential LA-ICPMS primary zircon standard if its variably high common Pb contents could be corrected for.

The same suite of analyses in Fig. 4A was reprocessed using Penglai zircon as the primary zircon standard and employing 91500 and Temora 2 zircon ($^{206}Pb/^{238}U$ TIMS age of 416.8 ± 1.3 Ma; Black et al., 2004) as secondary zircon standards. The VizualAge DRS of Petrus and Kamber (2012) yields strongly reversely discordant zircon data (Fig. 4B, 4C) for 91500 (Fig. 4B) and Temora 2 zircon (Fig. 4C) due to the variably high common Pb contents of the primary standard zircon. However when the VizualAge_UcomPbine DRS is employed with Penglai as the primary zircon standard, the 91500 and Temora 2 zircon standards yield ages of 1065 ± 6 Ma (Fig. 4D) and 419 ± 2 Ma (Fig. 4E). These data compare very favourably with existing U-Pb TIMS constraints on the 91500 and Temora 2 zircon standard, while the data are also strong empirical proof that the common Pb protocol works even on reference materials with large and variable incorporation of common Pb (Fig. 4A). Once corrected for common Pb, young primary zircon standards therefore appear to have strong potential in U-

Pb LA-ICPMS zircon dating studies as the absence of radiation-damage induced Pb loss results in highly concordant U-Pb data.

6. Conclusions

A data reduction scheme for Iolite (VizualAge_UcomPbine) is presented here for U-Pb LA-ICPMS dating of common Pb-bearing accessory minerals (e.g. apatite, titanite, allanite or rutile). The Iolite-based approach presents several advantages as i) it can employ any accessory mineral standard even if it incorporates variable amounts of common Pb and ii) it can be applied to raw data files from the vast majority of modern multi-collector and single-collector ICPMS instruments. It is thus ideally suited for LA-ICPMS laboratories wishing to set up a protocol for U-Pb dating of common Pb-bearing accessory minerals.

The DRS applies a common Pb correction to the user-selected age standard integrations and then fits session-wide "model" U-Pb fractionation curves to the time-resolved U-Pb standard data. This downhole fractionation model is applied to the unknowns and sample-standard bracketing (using a user-specified interpolation method) is used to calculate final isotopic ratios and ages. The DRS can undertake a common Pb-correction to the U-Pb reference standards using either the ^{204}Pb, ^{207}Pb or $^{208}Pb_{(no\ Th)}$ methods although a ^{207}Pb-based correction is preferred here. ^{204}Pb- and ^{208}Pb-corrected concordia diagrams and ^{204}Pb-, ^{207}Pb- and $^{208}Pb_{(no\ Th)}$-corrected age channels can be calculated for user-specified initial Pb ratio(s). All other conventional common Pb correction methods (e.g. intercept or isochron methods on co-genetic analyses) can be performed offline.

Strategies are presented for optimising the spread in radiogenic Pb ratios in co-genetic samples on concordia diagrams. These include using two separate co-magmatic phases from the same rock sample such as K-feldspar and a common-Pb bearing accessory mineral, or

two separate common Pb-bearing minerals (such as titanite and apatite). An alternative approach involves improving the spread in radiogenic Pb / common Pb ratios by analysing the same phase from two rock types of different composition. The standard data demonstrate the accuracy and precision that can be attained on the latest generation of Q-ICPMS instruments, with 2σ uncertainties of <1% on Phanerozoic apatite and titanite standards and 2σ uncertainties of <2% on Paleogene apatite and titanite standards. A range of LA-ICPMS U-Pb dating applications are also presented. These include U-Pb dating of apatite from Eoarchaean gneisses from Akilia Island, SW Greenland which host putative biogenic graphite inclusions and thus would represent the oldest indications of life on Earth; U-Pb apatite dating as a rapid method for determining the age of mafic intrusions; U-Pb common-Pb bearing accessory mineral dating of ash fall tuffs; producing temperature-time histories using multiple U-Pb thermochronometers and improving concordance in LA-ICPMS primary zircon standard datasets by analysing young, common Pb-bearing primary zircon standards that have not accumulated significant radiation damage.

Acknowledgements

Ray and Margaret Donelick of Apatite to Zircon, Inc. are thanked for supplying the Fish Canyon Tuff, McClure Mountain and Tioga samples and for many stimulating discussions on apatite U–Pb and trace element analyses by LA-ICPMS. Stuart Thomson is thanked for his advice on using McClure Mountain and Madagascar apatite as reference materials and for providing a crystal of Madagascar apatite. Craig Storey is thanked for supplying the Khan titanite standard. Allan Nutman is thanked for providing a split of sample G91-26. Thomas Zack is thanked for providing an aliquot of the R10 and R19b rutile standards. Tonny Thomsen and Kate Souders are thanked for providing data and samples which assisted in the

development of the ^{208}Pb common Pb correction. Chris McFarlane, Andrew Kylander-Clark and editor Klaus Mezger are thanked for their detailed reviews and suggestions which improved this manuscript.

Appendix A. VizualAge_UcomPbine DRS Outline

The DRS presented herein is based on the VizualAge DRS (Petrus and Kamber, 2012), which is in turn based on the U-Pb Geochronology DRS of Paton et al. (2010). The new DRS adds functionality by correcting the Pb composition of standard reference materials based on their known radiogenic and common Pb compositions, thus allowing standards which contain variable common Pb to be employed as primary reference materials in U-Pb geochronology studies. Baselines and standards are defined in the usual Iolite way, but this DRS differs from its predecessors by calculating ^{204}Pb-, ^{207}Pb- or $^{208}Pb_{(no\ Th)}$-based common Pb corrections for each time-slice of standard data. This correction is applied immediately after baseline subtraction and just prior to the calculation of "raw" standard ratios (i.e. before the downhole fractionation correction), as otherwise the downhole fractionation and mass bias corrections would be compromised by variable common Pb (e.g. Fig. 1). The methodology of how the ^{207}Pb correction is applied to a standard analysis is illustrated in Appendix Fig. A1. The discordia marked by the solid line passes through two standard analyses with variable common Pb. These two analyses exhibit no U/Pb elemental fractionation and so the lower concordia intercept is the true $^{238}U/^{206}Pb^*$ ratio of the standard. If these two standard analyses exhibited a constant U/Pb elemental fractionation, they too would lie on a discordia (marked by the dashed line on Fig. A1). Within-session drift in the U-Pb ratio is calculated from the ratio of this apparent lower concordia $^{238}U/^{206}Pb^*$ intercept to that of the true $^{238}U/^{206}Pb^*$ ratio of the standard.

Similar to the U-Pb Geochronology DRS of Paton et al. (2010) and the VizualAge DRS of Petrus and Kamber (2012), the appropriate index channel and reference material must be selected in the Edit Settings Dialog Box. Another dialog box then appears asking which common Pb correction method is to be used (^{204}Pb, ^{207}Pb, ^{208}Pb$_{(no\ Th)}$ or none) and whether the ratio corresponding to each time-slice of data or the average ratio for a given standard integration should be employed in the age calculations. If the DRS ultimately fails to display the down hole fractionation window then it can usually be launched by temporarily changing the "stats for baselines" option in the Edit Settings Dialog Box. Following the down hole fractionation correction, the common Pb-corrected primary standards are highlighted by a horizontal bar in the main window of the VizualAge_UcomPbine DRS to denote that the age channels of the primary reference material are now common Pb-corrected. A ^{207}Pb-corrected age channel ("Final207Age") or ^{208}Pb$_{(no\ Th)}$-corrected age channels can be calculated for unknowns using user-specified initial ^{207}Pb/^{206}Pb and ^{208}Pb/^{206}Pb ratios. The correction is calculated significantly faster if the Final207Age or Final208noTh age channels are not viewed when the correction is launched. If the ^{207}Pb- or ^{208}Pb$_{(no\ Th)}$-corrected ages are not visible in the Iolite data reports or in the exported data files, it is recommended that the appropriate final age channel is viewed with the relevant active integration type selected. ^{204}Pb- and ^{208}Pb-corrected Wetherill and Tera-Wasserburg concordia diagrams can also be viewed in the VizualAge Concordia menu using the FinalPbC and FinalNoTh options respectively.

When using the ^{207}Pb-based routine, each segment of time-resolved standard data is corrected as follows:

$$^{207}\mathrm{Pb}_r = {}^{207}\mathrm{Pb}_m - {}^{206}\mathrm{Pb}_m \times \left(\frac{^{207}\mathrm{Pb}}{^{206}\mathrm{Pb}}\right)_c \times \mathrm{f}_{206} \quad (1)$$

and

$$^{206}\mathrm{Pb}_r = {}^{206}\mathrm{Pb}_m \times (1 - \mathrm{f}_{206}), \quad (2)$$

where

$$f_{206} = \frac{\left(\frac{^{207}\mathrm{Pb}}{^{206}\mathrm{Pb}}\right) - \left(\frac{^{207}\mathrm{Pb}}{^{206}\mathrm{Pb}}\right)_r}{\left(\frac{^{207}\mathrm{Pb}}{^{206}\mathrm{Pb}}\right)_c - \left(\frac{^{207}\mathrm{Pb}}{^{206}\mathrm{Pb}}\right)_r} \quad (3)$$

and the subscripts m, r, and c represent measured, radiogenic and common, respectively. The values for the radiogenic and common Pb ratios are retrieved from the appropriate Iolite standard file. If the ^{204}Pb based routine is used, the correction applied is as follows:

$$^{206}\mathrm{Pb}_r = {}^{206}\mathrm{Pb}_\mathrm{m} \times \left[\frac{\left(\frac{^{206}\mathrm{Pb}}{^{204}\mathrm{Pb}}\right)_\mathrm{m} - \left(\frac{^{206}\mathrm{Pb}}{^{204}\mathrm{Pb}}\right)_\mathrm{c}}{\left(\frac{^{206}\mathrm{Pb}}{^{204}\mathrm{Pb}}\right)_\mathrm{m}}\right] \quad (4)$$

$$^{207}\mathrm{Pb}_r = {}^{207}\mathrm{Pb}_\mathrm{m} \times \left[\frac{\left(\frac{^{207}\mathrm{Pb}}{^{204}\mathrm{Pb}}\right)_\mathrm{m} - \left(\frac{^{207}\mathrm{Pb}}{^{204}\mathrm{Pb}}\right)_\mathrm{c}}{\left(\frac{^{207}\mathrm{Pb}}{^{204}\mathrm{Pb}}\right)_\mathrm{m}}\right] \quad (5)$$

where the subscripts have the same meaning as above. Assuming no Th (and hence no radiogenic ^{208}Pb) is present, then the ^{208}Pb correction is analogous to the ^{204}Pb correction, with ^{208}Pb replacing ^{204}Pb in equations 4 and 5. Upon completion of the common Pb correction routine, the DRS proceeds as outlined in Petrus and Kamber (2012).

References

Black, L.P., Kamo, S.L., Allen, C.M., Aleinikoff, J.N., Davis, D.W., Korsch, R.J., Foudoulis, C., 2003. TEMORA 1: a new zircon standard for Phanerozoic U-Pb geochronology. Chemical Geology, 200(1-2): 155-170.

Black, L.P., Kamo, S.L., Allen, C.M., Davis, D.W., Aleinikoff, J.N., Valley, J.W., Mundil, R., Campbell, I.H., Korsch, R.J., Williams, I.S., Foudoulis, C., 2004. Improved $^{206}Pb/^{238}U$ microprobe geochronology by the monitoring of a trace-element-related matrix effect; SHRIMP, ID–TIMS, ELA–ICP–MS and oxygen isotope documentation for a series of zircon standards. Chemical Geology 205, 115–140.

Chamberlain, K.R., Bowring, S.A., 2000. Apatite-feldspar U-Pb thermochronometer: A reliable, mid-range (450 °C), diffusion-controlled system. Chemical Geology, 172(1-2): 173-200.

Chambers, L.M., Pringle, M.S., 2001. Age and duration of activity at the Isle of Mull Tertiary igneous centre, Scotland, and confirmation of the existence of subchrons during Anomaly 26r. Earth and Planetary Science Letters, 193(3-4): 333-345.

Cherniak, D.J., 1993. Lead diffusion in titanite and preliminary results on the effects of radiation damage on Pb transport. Chemical Geology, 110(1): 177-194.

Cherniak, D.J., Lanford, W.A., Ryerson, F.J., 1991. Lead Diffusion in Apatite and Zircon Using Ion-Implantation and Rutherford Backscattering Techniques. Geochimica Et Cosmochimica Acta, 55(6): 1663-1673.

Chew, D.M., Donelick, R.A., 2012. Combined apatite fission track and U-Pb dating by LA-ICPMS and future trends in apatite provenance analysis. In: Sylvester, P. (Ed.), Quantitative Mineralogy and Microanalysis of Sediments and Sedimentary Rocks. Mineralogical Association of Canada, pp. 219-248.

Chew, D.M., Schaltegger, U., Košler, J., Whitehouse, M.J., Gutjahr, M., Spikings, R.A., Miškovic, A., 2007. U-Pb geochronologic evidence for the evolution of the

Gondwanan margin of the north-central Andes. Geological Society of America Bulletin., 119(5/6): 697-711.

Chew, D.M., Schaltegger, U., Miškovic, A., Fontignie, D., Frank, M., 2005. Deciphering the tectonic evolution of the Peruvian segment of the Gondwanan margin, 6th International Symposium on Andean Geodynamics (ISAG 2005, Barcelona), Extended Abstracts, pp. 166–169.

Chew, D.M., Sylvester, P.J., Tubrett, M.N., 2011. U-Pb and Th-Pb dating of apatite by LA-ICPMS. Chemical Geology, 280(1-2): 200-216.

Cocherie, A., 2009. Common-Pb correction in laser U-Pb geochronology using MC-ICPMS and a multi-ion counting system. Geochimica et Cosmochimica Acta, 73(13): A233-A233.

Cochrane, R., Spikings, R.A., Chew, D., Wotzlaw, J.-F., Chiaradia, M., Tyrrell, S., Schaltegger, U., Van der Lelij, R., submitted. Isotopic closure, volume diffusion and high temperature thermal histories of crustal rocks. Geochimica et Cosmochimica Acta.

Cottle, J.M., Kylander-Clark, A.R., Vrijmoed, J.C., 2012. U-Th/Pb geochronology of detrital zircon and monazite by single shot laser ablation inductively coupled plasma mass spectrometry (SS-LA-ICPMS). Chemical Geology, 332: 136-147.

Eggins, S.M., Kinsley, L.P.J., Shelley, J.M.G., 1998. Deposition and element fractionation processes during atmospheric pressure laser sampling for analysis by ICP-MS. Applied Surface Science, 127: 278-286.

Eggins, S.M., Woodhead, J.D., Kinsley, L.P.J., Mortimer, G.E., Sylvester, P., McCulloch, M.T., Hergt, J.M., Handler, M.R., 1997. A simple method for the precise determination of >=40 trace elements in geological samples by ICPMS using enriched isotope internal standardisation. Chemical Geology, 134(4): 311-326.

Gehrels, G.E., Valencia, V.A., Ruiz, J., 2008. Enhanced precision, accuracy, efficiency, and spatial resolution of U-Pb ages by laser ablation-multicollector-inductively coupled plasma-mass spectrometry. Geochemistry Geophysics Geosystems, 9.

Gibson, G.M., Ireland, T.R., 1996. Extension of Delamerian (Ross) orogen into western New Zealand: Evidence from zircon ages and implications for crustal growth along the Pacific margin of Gondwana. Geology, 24(12): 1087-1090.

Gregory, C.J., Rubatto, D., Allen, C.M., Williams, I.S., Hermann, J., Ireland, T., 2007. Allanite micro-geochronology: A LA-ICP-MS and SHRIMP U-Th-Pb study. Chemical Geology, 245(3-4): 162-182.

Heaman, L.M., 2009. The application of U-Pb geochronology to mafic, ultramafic and alkaline rocks: An evaluation of three mineral standards. Chemical Geology, 261(1-2): 42-51.

Hellstrom, J.C., Paton, C., Woodhead, J.D., Hergt, M., 2008. Iolite: Software for spatially resolved LA-(quad and MC) ICP-MS analysis. In: Sylvester, P. (Ed.), Laser ablation ICP-MS in the Earth sciences: Current practices and outstanding issues Mineralogical Association of Canada, Short course, pp. 343-348.

Hemming, S.R., Rasbury, E.T., 2000. Pb isotope measurements of sanidine monitor standards: implications for provenance analysis and tephrochronology. Chemical Geology, 165(3): 331-337.

Hodges, K.V., Harries, W.E., Bowring, S.A., 1994. 40Ar/39Ar age gradients in micas from a high-temperature-low-pressure metamorphic terrain: Evidence for very slow cooling and implications for the interpretation of age spectra. Geology, 22(1): 55-58.

Hoskin, P.W.O., Schaltegger, U., 2003. The composition of zircon and igneous and metamorphic petrogenesis. In: Hanchar, J.M., Hoskin, P.W.O. (Eds.), Zircon.

Reviews in Mineralogy and Geochemistry. Mineralogical Society of America, pp. 27-62.

Jackson, S.E., Longerich, H.P., Horn, I., Dunning, R., 1996. The application of laser ablation microprobe (LAM)-ICP-MS to in situ U–Pb zircon geochronology. Journal of Conference Abstracts, 1: 283.

Kennedy, A.K., Kamo, S.L., Nasdala, L., Timms, N.E., 2010. Grenville Skarn Titanite: potential reference material for SIMS U–Th–Pb analysis. The Canadian Mineralogist, 48(6): 1423-1443.

Kinny, P.D., Compston, W., Williams, I.S., 1991. A reconnaissance ion-probe study of hafnium isotopes in zircons. Geochimica et Cosmochimica Acta 55, 849– 859.

Kohn, M.J., Corrie, S.L., 2011. Preserved Zr-temperatures and U-Pb ages in high-grade metamorphic titanite: Evidence for a static hot channel in the Himalayan orogen. Earth and Planetary Science Letters, 311(1-2): 136-143.

Košler, J., Fonneland, H., Sylvester, P., Tubrett, M., Pedersen, R.B., 2002. U-Pb dating of detrital zircons for sediment provenance studies - a comparison of laser ablation ICPMS and SIMS techniques. Chemical Geology, 182(2-4): 605-618.

Košler, J., Sylvester, P.J., 2003. Present trends and the future of zircon in geochronology: laser ablation ICPMS. In: Hanchar, J.M., Hoskin, P.W.O. (Eds.), Zircon. Reviews in Mineralogy and Geochemistry, pp. 243-275.

Košler, J., Tubrett, M.N., Sylvester, P.J., 2001. Application of laser ablation ICP-MS to U-Th-Pb dating of monazite. Geostandards Newsletter - the Journal of Geostandards and Geoanalysis, 25(2-3): 375-386.

Kramers, J.D., Tolstikhin, I.N., 1997. Two terrestrial lead isotope paradoxes, forward transport modelling, core formation and the history of the continental crust. Chemical Geology, 139(1-4): 75-110.

Krogh, T.E., Davis, G.L., 1974. Alteration in zircons with discordant U–Pb ages. Carnegie Inst. Yearbook 73, 560– 567.

Krogh, T.E., Davis, G.L., 1975. Alteration in zircons and differential dissolution of altered and metamict zircon. Carnegie Inst. Yearbook 74, 619– 623.

Kuiper, K.F., Deino, A., Hilgen, F.J., Krijgsman, W., Renne, P.R., Wijbrans, J.R., 2008. Synchronizing rock clocks of Earth history. Science, 320(5875): 500-504.

Lepland, A., van Zuilen, M.A., Arrhenius, G., Whitehouse, M.J., Fedo, C.M., 2005. Questioning the evidence for Earth's earliest life—Akilia revisited. Geology, 33(1): 77-79.

Luvizotto, G.L., Zack, T., Meyer, H.P., Ludwig, T., Triebold, S., Kronz, A., Münker, C., Stockli, D.F., Prowatke, S., Klemme, S., Jacob, D.E., von Eynatten, H., 2009, Rutile crystals as potential trace element and isotope mineral standards for microanalysis. Chemical Geology, 261 (3–4): 346-369.

McDougall, I., Harrison, T.M., 1999. Geochronology and Thermochronology by the 40Ar/39Ar Method. Oxford University Press, 269 pp.

Li, X.H., Long, W.G., Li, Q.L., Liu, Y., Zheng, Y.F., Yang, Y.H., Chamberlain, K.R., Wan, D.F., Guo, C.H., Wang, X.C., Tao, H., 2010. Penglai Zircon Megacrysts: A Potential New Working Reference Material for Microbeam Determination of Hf-O Isotopes and U-Pb Age. Geostandards and Geoanalytical Research, 34(2): 117-134.

Ludwig, K.R., 1998. On the treatment of concordant uranium-lead ages. Geochimica et Cosmochimica Acta, 62(4): 665-676.

Mattinson, J.M., 2005. Zircon U-Pb chemical abrasion ("CA-TIMS") method: Combined annealing and multi-step partial dissolution analysis for improved precision and accuracy of zircon ages. Chemical Geology, 220(1-2): 47-66.

McDowell, F.W., McIntosh, W.C., Farley, K.A., 2005. A precise ^{40}Ar-^{39}Ar reference age for the Durango apatite (U-Th)/He and fission-track dating standard. Chemical Geology, 214(3-4): 249-263.

McFarlane, C.R.M., Luo, Y., 2012. U-Pb Geochronology Using 193 nm Excimer LA-ICP-MS Optimized for In Situ Accessory Mineral Dating in Thin Sections. Geoscience Canada, 39: 158-+.

Mojzsis, S.J., Arrhenius, G., McKeegan, K.D., Harrison, T.M., Nutman, A.P., Friend, C.R.L., 1996. Evidence for life on Earth before 3,800 million years ago. Nature, 384(6604): 55-59.

Myers, J.S., Crowley, J.L., 2000. Vestiges of life in the oldest Greenland rocks? A review of early Archean geology in the Godthåbsfjord region, and reappraisal of field evidence for> 3850 Ma life on Akilia. Precambrian Research, 103(3): 101-124.

Nutman, A.P., Mojzsis, S.J., Friend, C.R.L., 1997. Recognition of≥ 3850 Ma water-lain sediments in West Greenland and their significance for the early Archaean Earth. Geochimica et Cosmochimica Acta, 61(12): 2475-2484.

Paton, C., Hellstrom, J., Paul, B., Woodhead, J., Hergt, J., 2011. Iolite: Freeware for the visualisation and processing of mass spectrometric data. Journal of Analytical Atomic Spectrometry, 26(12): 2508-2518.

Paton, C., Woodhead, J.D., Hellstrom, J.C., Hergt, J.M., Greig, A., Maas, R., 2010. Improved laser ablation U-Pb zircon geochronology through robust downhole fractionation correction. Geochemistry Geophysics Geosystems, 11.

Petrus, J.A., Kamber, B.S., 2012. VizualAge: A Novel Approach to Laser Ablation ICP-MS U-Pb Geochronology Data Reduction. Geostandards and Geoanalytical Research, 36(3): 247-270.

Piccoli, P.M., Candela, P.A., 2002. Apatite in igneous systems. In: Kohn, M.L., Rakovan, J., Hughes, J.M. (Eds.), Phosphates: Geochemical, Geobiological and Materials Importance. Reviews in Mineralogy and Geochemistry. Reviews in Mineralogy and Geochemistry, pp. 255-292.

Roden, M.K., Parrish, R.R., Miller, D.S., 1990. The absolute age of the Eifelian Tioga ash bed, Pennsylvania. The Journal of Geology, 98: 282-285.

Sano, Y., Terada, K., Takahashi, Y., Nutman, A.P., 1999. Origin of life from apatite dating? Nature, 400(6740): 127-127.

Schoene, B., Bowring, S.A., 2006. U-Pb systematics of the McClure Mountain syenite: thermochronological constraints on the age of the Ar-40/Ar-39 standard MMhb. Contributions to Mineralogy and Petrology, 151(5): 615-630.

Schoene, B., Bowring, S.A., 2007. Determining accurate temperature-time paths from U-Pb thermochronology: An example from the Kaapvaal craton, southern Africa. Geochimica et Cosmochimica Acta, 71(1): 165-185.

Scott, D.J., St-Onge, M.R., 1995. Constraints on Pb closure temperature in titanite based on rocks from the Ungava orogen, Canada: Implications for U-Pb geochronology and PTt path determinations. Geology, 23(12): 1123-1126.

Simonetti, A., Heaman, L.M., Chacko, T., Banerjee, N.R., 2006. In situ petrographic thin section U-Pb dating of zircon, monazite, and titanite using laser ablation-MC-ICP-MS. International Journal of Mass Spectrometry, 253(1-2): 87-97.

Slama, J., Košler, J., Condon, D.J., Crowley, J.L., Gerdes, A., Hanchar, J.M., Horstwood, S.A., M., Morris, G.A., Nasdala, L., Norberg, N., Schaltegger, U., Schoene, B., Tubrett, M.N., Whitehouse, M.J., 2008. Plešovice zircon – a new natural reference material for U-Pb and Hf isotopic microanalysis. Chemical Geology, 249(1-2): 1-35.

Spencer, K.J., Hacker, B.R., Kylander-Clark, A.R.C., Andersen, T.B., Cottle, J.M., Stearns, M.A., Poletti, J.E., Seward, G.G.E., 2013. Campaign-style titanite U-Pb dating by laser-ablation ICP: Implications for crustal flow, phase transformations and titanite closure. Chemical Geology, 341: 84-101.

Stacey, J.S., Kramers, J.D., 1975. Approximation of terrestrial lead isotope evolution by a two-stage model. Earth and Planetary Science Letters, 26(2): 207-221.

Storey, C.D., Smith, M.P., Jeffries, T.E., 2007. In situ LA-ICP-MS U-Pb dating of metavolcanics of Norrbotten, Sweden: Records of extended geological histories in complex titanite grains. Chemical Geology, 240(1-2): 163-181.

Sun, J.F., Yang, J.H., Wu, F.Y., Xie, L.W., Yang, Y.H., Liu, Z.C., Li, X.H., 2012. In situ U-Pb dating of titanite by LA-ICPMS. Chinese Science Bulletin, 57(20): 2506-2516.

Sylvester, P.J., Ghaderi, M., 1997. Trace element analysis of scheelite by excimer laser ablation inductively coupled plasma mass spectrometry (ELA-ICP-MS) using a synthetic silicate glass standard. Chemical Geology, 141(1-2): 49-65.

Thomson, S.N., Gehrels, G.E., Ruiz, J., Buchwaldt, R., 2012. Routine low-damage apatite U-Pb dating using laser ablation-multicollector-ICPMS. Geochemistry Geophysics Geosystems, 13.

Tucker, R.D., Bradley, D.C., Ver Straeten, C.A., Harris, A.G., Ebert, J.R., McCutcheon, S.R., 1998. New U–Pb zircon ages and the duration and division of Devonian time. Earth and Planetary Science Letters, 158(3): 175-186.

Whitehouse, M.J., Fedo, C.M., 2003. Deformation features and critical field relationships of early Archaean rocks, Akilia, southwest Greenland. Precambrian Research, 126(3): 259-271.

Whitehouse, M.J., Kamber, B.S., 2005. Assigning dates to thin gneissic veins in high-grade metamorphic terranes: a cautionary tale from Akilia, southwest Greenland. Journal of Petrology, 46(2): 291-318.

Whitehouse, M.J., Myers, J.S., Fedo, C.M., 2009. The Akilia Controversy: field, structural and geochronological evidence questions interpretations of> 3.8 Ga life in SW Greenland. Journal of the Geological Society, 166(2): 335-348.

Wiedenbeck, M., Alle, P., Corfu, F., Griffin, W.L., Meier, M., Oberli, F., von Quadt, A., Roddick, J.C., Spiegel, W., 1995. Three natural zircon standards for U-Th-Pb, Lu-Hf, trace element and REE analyses. Geostandards Newsletter, 19(1): 1-23.

Williams, I.S., 1998. U-Th-Pb geochronology by ion microprobe. In: McKibben, M.A., Shanks III, W.C., Ridley, W.I. (Eds.), Applications of microanalytical techniques to understanding mineralizing processes. Reviews in Economic Geology, pp. 1–35.

Woodhead, J.D., Hellstrom, J., Paton, C., Hergt, J.M., Greig, A., Mass, R., 2008. A guide to depth profiling and imaging applications of ICP-MS. In: Sylvester, P. (Ed.), Laser ablation ICP-MS in the Earth sciences: Current practices and outstanding issues. Mineralogical Association of Canada, Short Course Series, pp. 135-145.

Zack, T., Stockli, D.F., Luvizotto, G.L., Barth, M.G., Belousova, E., Wolfe, M.R., Hinton, R.W., 2011. In situ U-Pb rutile dating by LA-ICP-MS: ^{208}Pb correction and prospects for geological applications. Contributions to Mineralogy and Petrology, 162(3): 515-530.

Figure captions

Figure 1 A). Time-resolved ^{207}Pb/^{235}U downhole signal collected from single-spot ablations (40 μm) of McClure Mountain apatite without any common Pb-correction. B) Time-resolved

$^{207}Pb/^{235}U$ downhole signal collected from single-spot ablations (50 μm) of McClure Mountain apatite corrected for common Pb using a ^{207}Pb correction.

Figure 2 (A-D). Tera-Wasserburg U-Pb lower intercept ages anchored through common Pb for the apatite and titanite standards analysed in this study using Madagascar apatite (Thomson et al., 2012) and OLT1 titanite (Kennedy et al., 2010) as primary standards. Weighted average ^{207}Pb-corrected ages are presented as insets in each figure. (E) Wetherill concordia lower intercept age anchored through common Pb for Durango apatite with the ^{204}Pb-corrected concordia age as an inset. (F) Tera-Wasserburg concordia lower intercept age anchored through common Pb for Ben Lawers rutile with the $^{208}Pb_{(no\ Th)}$-corrected Tera-Wasserburg concordia age as an inset.

Figure 3 (A-B). Tera-Wasserburg lower intercept U-Pb ages anchored through common Pb for apatite unknowns. (C) Tera-Wasserburg lower intercept U-Pb age for Fish Canyon Tuff constrained by the large spread in radiogenic Pb ratio between co-magmatic apatite and titanite. (D) Tera-Wasserburg lower intercept U-Pb titanite age for samples DC 4/5/1 and DC 4/5/2 constrained by the large spread in radiogenic Pb ratio between the consanguineous samples. (E) Tera-Wasserburg lower intercept U-Pb apatite age for samples DC 4/5/2 anchored by the Pb isotopic composition of co-magmatic K-feldspar. (F) Temperature – time history for sample DC 4/5/2 derived from LA-ICPMS U-Pb zircon, titanite and apatite dating and LA-ICPMS apatite fission track analyses. (G) apatite core-rim ^{207}Pb-corrected U-Pb age profiles from Akilia Island, SW Greenland.

Figure 4 (A). Tera-Wasserburg U-Pb unanchored lower intercept age for Penglai zircon using 91500 as the primary zircon standard. (B-C). Tera-Wasserburg U-Pb age data for 91500 (B) and Temora-2 (C) zircon using Penglai zircon as the primary standard uncorrected for common Pb. (D-E). Tera-Wasserburg U-Pb concordia ages for 91500 (D) and Temora-2 (E)

zircon using Penglai zircon as the primary standard and corrected for common Pb using the new VizualAge_UcomPbine DRS.

Appendix Figure A1. Tera-Wasserburg U-Pb lower concordia diagram illustrating the ^{207}Pb correction methodology and the effects of U-Pb elemental fractionation.

Figure 1

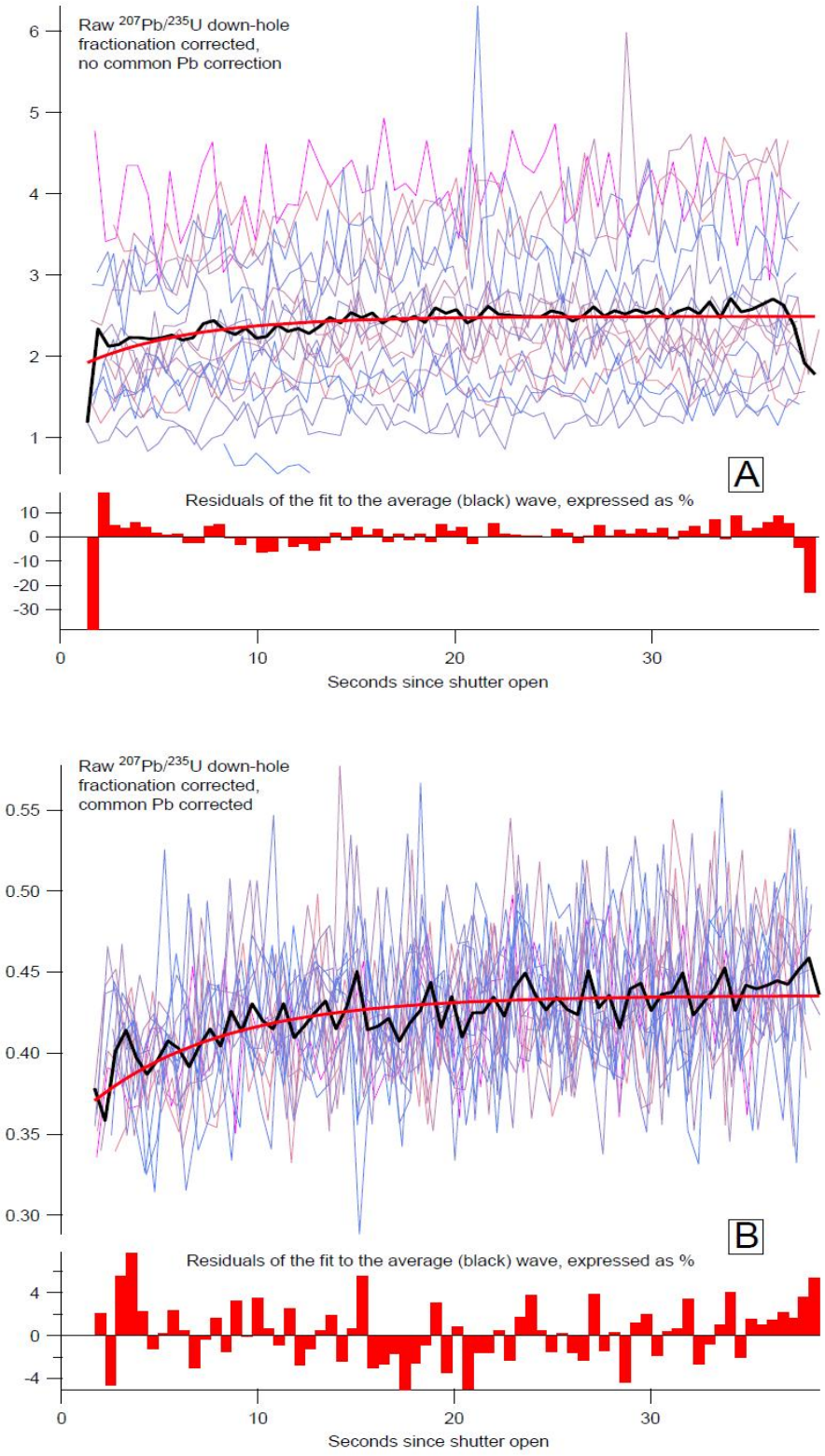

Figure 2

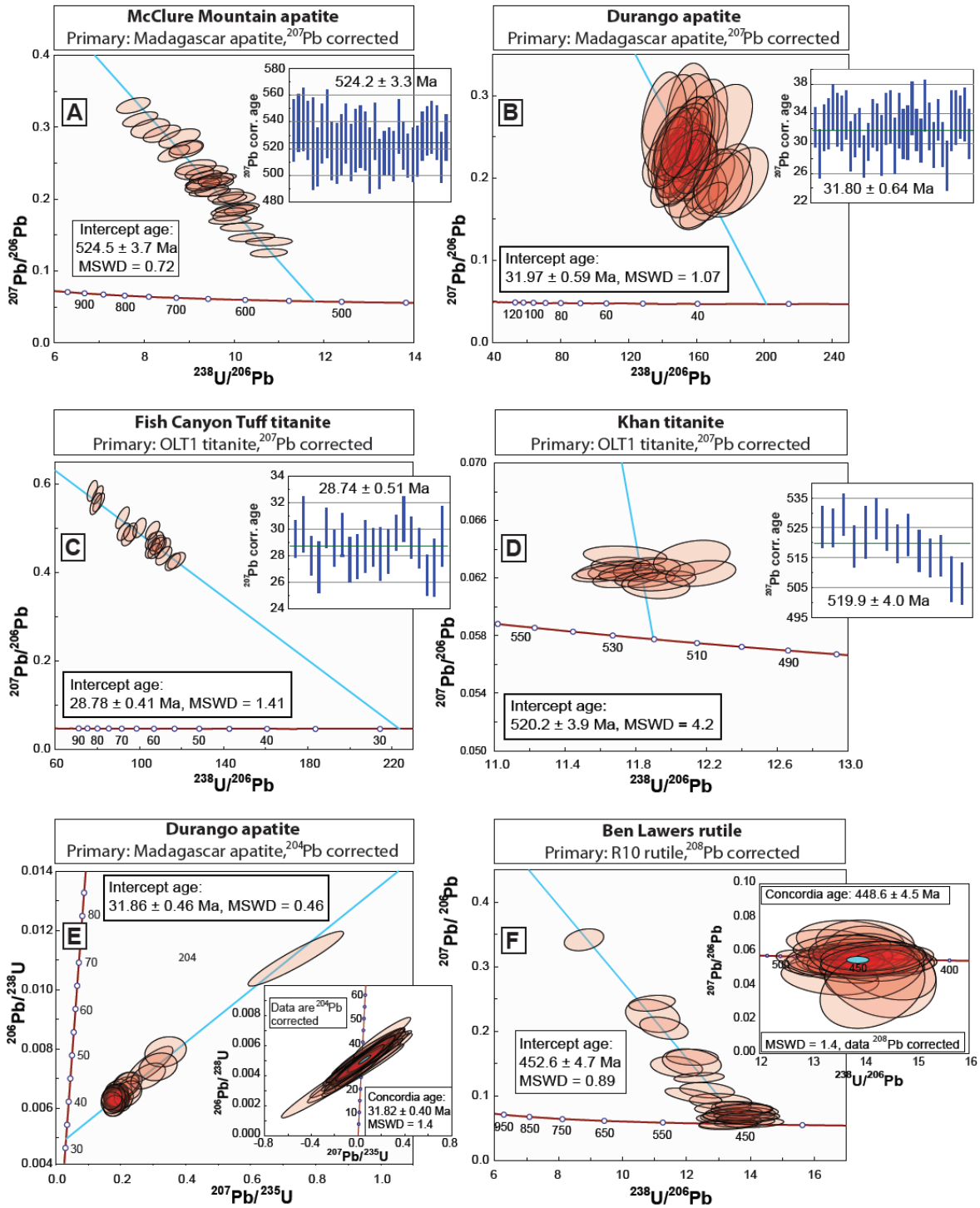

Figure 3

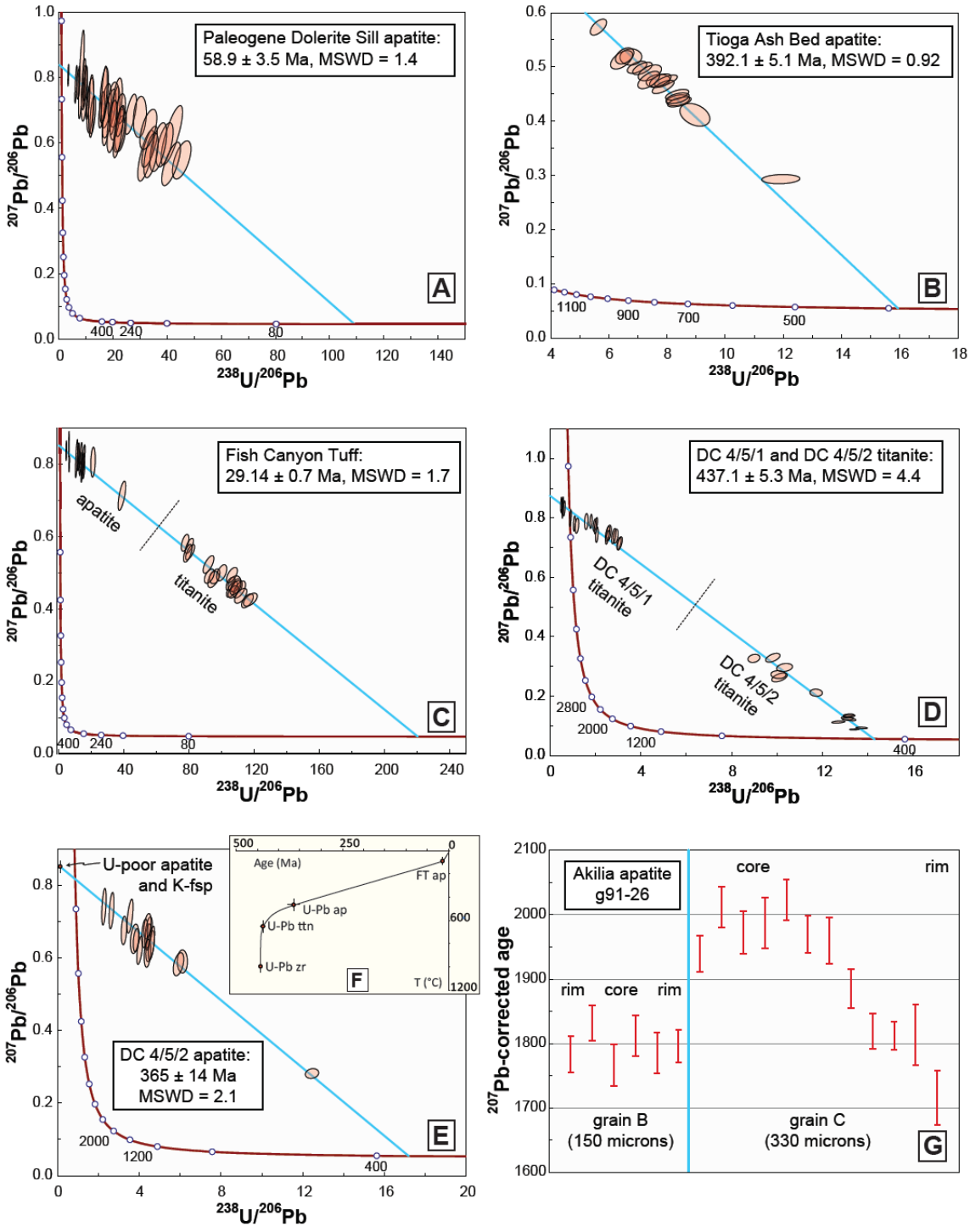

Figure 4

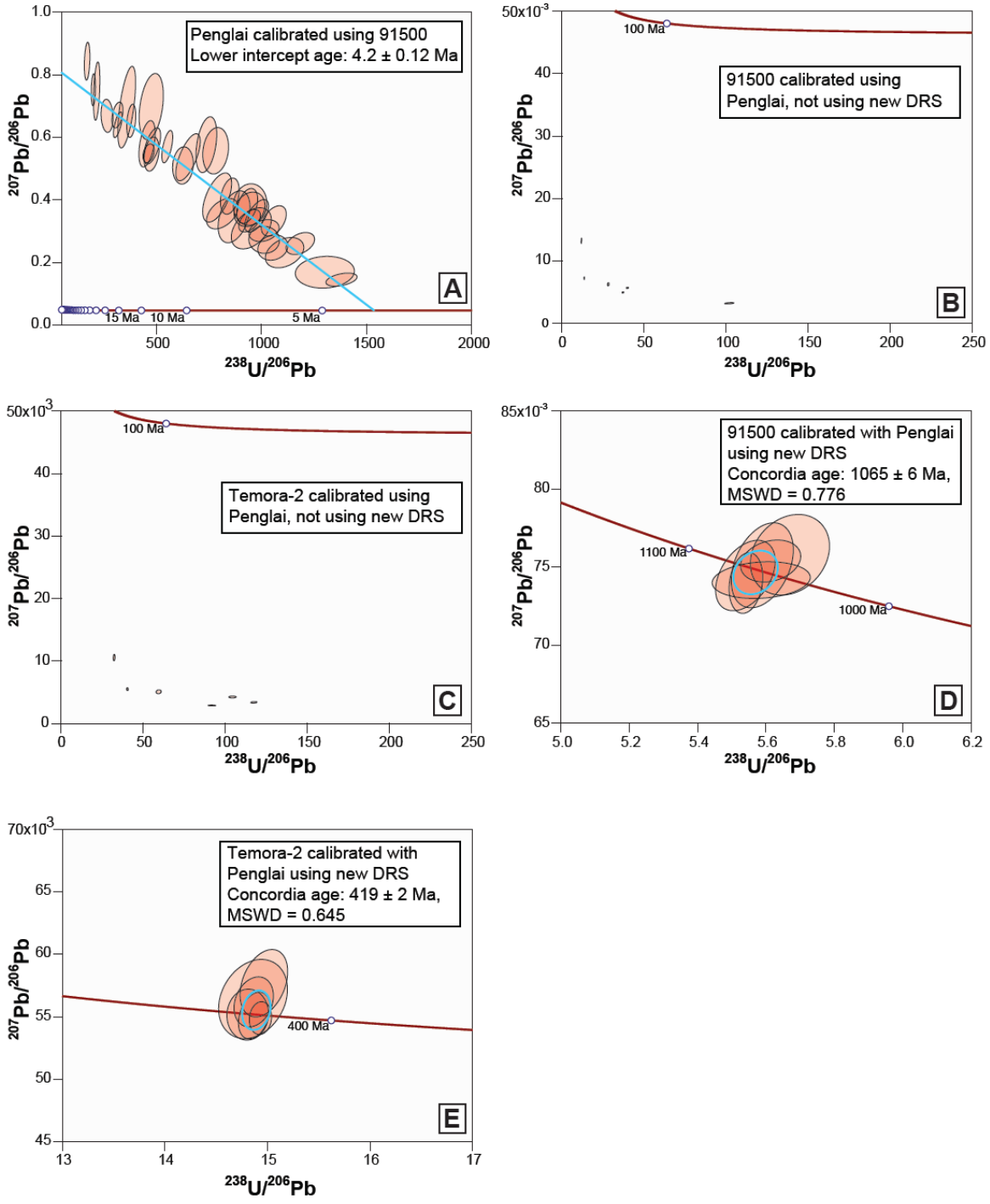

Appendix Figure A1

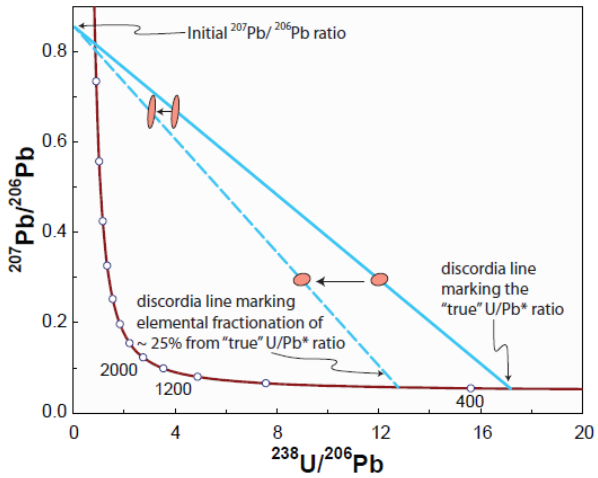

Table 1. Analytical parameters for different sessions

	All U-Pb apatite and titanite standards	U-Pb apatite fission track samples	U-Pb rutile analyses	U-Pb zircon standards
Laser parameters				
Instrument	Photon Machines Analyte Exite ArF Excimer 193 nm	Photon Machines Analyte Exite ArF Excimer 193 nm	Photon Machines Analyte Exite ArF Excimer 193 nm	Resonetics RESOlution M-50 (ArF Excimer 193 nm)
Washout	25 s (60 s for ^{204}Pb-correction)	25s	15 s	15 s
Background	15 s (50 s for ^{204}Pb correction)	15 s	15 s	15 s
Analysis duration	45 s	45 s	35 s	30 s
Laser repetition rate	4.0 Hz	4.0 Hz	5.0 Hz	5.0 Hz
Spot size	24, 50 or 130 micron diameter	30 micron diameter	80 micron diameter spot	60 micron diameter spot
Attenuation	0.28	0.28	0.28	0.5
Energy	3.31 J/cm^2	3.31 J/cm^2	3.31 J/cm^2	7 J/cm^2
Carrier gas 1	*800 mL/min He*	*800 mL/min He*	*800 mL/min He*	*700 mL/min He*
Carrier gas 2	*200 mL/min He*	*200 mL/min He*	*200 mL/min He*	*6 mL/min N2*
Mass spectrometer parameters				
Instrument	Thermo Scientific iCAP Qs	Thermo Scientific iCAP Qs	Thermo Scientific iCAP Qs	Thermo Scientific X Series II
Plasma RF power	1450 W	1450 W	1450 W	1400 W
Plasma carrier gas flow	0.85 L/min	0.85 L/min	0.85 L/min	0.7 L/min
Isotopic and sample information				
Number of isotopes measured	9	26	8	9
Total analysis time per cycle	0.543 (24 & 50 microns), 0.395 (130 microns	0.39	0.465	0.243
Isotopes measured (in analysis order)	^{43}Ca, ^{200}Hg, ^{202}Hg, ^{204}Pb, ^{206}Pb, ^{207}Pb, ^{208}Pb, ^{232}Th, ^{238}U	^{31}P, ^{35}Cl, ^{43}Ca, ^{86}Sr, ^{93}Nb, ^{139}La, ^{140}Ce, ^{141}Pr, ^{146}Nd, ^{147}Sm, ^{153}Eu, ^{157}Gd, ^{159}Tb, ^{163}Dy, ^{165}Ho, ^{166}Er, ^{169}Tm, ^{172}Yb, ^{175}Lu, ^{200}Hg, ^{204,206,207,208}Pb, ^{232}Th, ^{238}U	^{49}Ti, ^{202}Hg, ^{204}Hg+Pb, ^{206}Pb, ^{207}Pb, ^{208}Pb, ^{232}Th, ^{238}U	^{91}Zr, ^{200}Hg, ^{202}Hg, ^{204}Hg+Pb, ^{206}Pb, ^{207}Pb, ^{208}Pb, ^{232}Th, ^{238}U

Table 2
Summary of apatite, titanite and rutile age and concentration data

Sample	Th	U	Pb	Th/U	n	$^{207}Pb/^{206}Pb_i$	How is $^{207}Pb/^{206}Pb_i$ constrained?	Primary standard	Concordia Intercept	MSWD	2σ %	Pb-corrected age	Correction method	MSWD	2σ %
McClure Mountain apatite	58	19.6	6.7	3.0	33	0.8820	Total U-Pb isochron	Madagascar apatite, ^{207}Pb corr.	524.5 ± 3.7 Ma	0.72	0.7%	524.6 ± 3.2 Ma	^{207}Pb-corr. weighted mean	2.50	0.6%
Durango apatite	270	14.5	0.3	18.58	36	0.8376	Stacey & Kramers (31.44 Ma)	Madagascar apatite, ^{207}Pb corr.	31.97 ± 0.59 Ma	1.07	1.8%	32.20 ± 0.51 Ma	^{207}Pb-corr. weighted mean	1.04	1.6%
Durango apatite	270	14.5	0.3	18.58	36	0.8376	Stacey & Kramers (31.44 Ma)	Madagascar apatite, ^{204}Pb corr.	31.86 ± 0.46 Ma	0.46	1.4%	31.82 ± 0.40 Ma	^{204}Pb-corr. Concordia	1.4	1.3%
Fish Canyon Tuff titanite	343	66.8	2.1	5.1	20	0.8444	Pb isotopic composition of sanidine	OLT1 titanite, ^{207}Pb corr.	28.78 ± 0.41 Ma	1.41	1.4%	28.75 ± 0.5 Ma	^{207}Pb-corr. weighted mean	2.0	1.8%
Khan titanite	567	732	209.6	2.71	14	0.8714	Stacey & Kramers (522.2 Ma)	OLT1 titanite, ^{207}Pb corr.	520.2 ± 3.9 Ma	4.2	0.7%	520.7 ± 3.8 Ma	^{207}Pb-corr. weighted mean	14	0.7%
Ben Lawers rutile	0.0001	4.1	0.6	0.0003	29	0.8663	Stacey & Kramers (450 Ma)	R10 rutile, ^{208}Pb corr.	452.6 ± 4.7 Ma	0.89	1.0%	448.6 ± 4.5 Ma	^{208}Pb-corr. TW Concordia	1.40	1.0%
Palaeogene dolerite sill apatite	14.9	5.6	1.3	2.66	40	0.8394	Stacey & Kramers (58.9 Ma)	Madagascar apatite, ^{207}Pb corr.	58.9 ± 3.5 Ma	1.4	5.9%	58.1 ± 4.0 Ma	^{207}Pb-corr. weighted mean	1.6	6.9%
Tioga Ash Bed apatite	7.0	33.4	14.9	0.21	18	0.8620	Stacey & Kramers (392.1 Ma)	Madagascar apatite, ^{207}Pb corr.	392.1 ± 5.1 Ma	0.92	1.3%	391.0 ± 4.9 Ma	^{207}Pb-corr. weighted mean	2.5	1.3%
Fish Canyon Tuff apatite# and titanite	50.0	13.1	3.7	3.82	37	0.8444	constrained by apatite and titanite data*	Madagascar apatite, ^{207}Pb corr.	29.14 ± 0.7 Ma	1.7	2.4%	28.7 ± 0.51 Ma	^{207}Pb-corr. weighted mean	2.2	1.8%
DC 4/5/1 titanite	0.5	2.0	3.8	0.23	19	0.8570	constrained by DC 4/5/1, 4/5/2 titanite*	OLT1 titanite, ^{207}Pb corr.	437.1 ± 5.3 Ma	4.4	1.2%	435.2 ± 5.0 Ma	^{207}Pb-corr. weighted mean	8.0	1.1%
DC 4/5/2 titanite	9.2	50.0	13.5	0.18	13	0.8570	constrained by DC 4/5/1, 4/5/2 titanite*	OLT1 titanite, ^{207}Pb corr.	437.1 ± 5.3 Ma	4.4	1.2%	435.2 ± 5.0 Ma	^{207}Pb-corr. weighted mean	8.0	1.1%
DC 4/5/2 apatite	8.9	10.4	8.2	0.86	17	0.8570	Pb isotopic composition of K-feldspar	Madagascar apatite, ^{207}Pb corr.	365 ± 14 Ma	2.1	3.8%	366 ± 14 Ma	^{207}Pb-corr. weighted mean	2.4	3.8%

All errors are quoted at the 2σ level. Concordia Intercept denotes a Tera-Wasserburg or Wetherill lower intercept age anchored through $^{207}Pb/^{206}Pb_i$ with the exception of samples marked with an asterisk which do not assume any initial Pb constraints. The Pb-corrected ages also use the $^{207}Pb/^{206}Pb_i$ values. #The Th, U and Pb concentrations in the Fish Canyon Tuff apatite and titanite sample refer to the apatite data.

Highlights

- General approach to U–Pb LA-ICPMS dating of common Pb-bearing minerals using Iolite
- The method can use any accessory mineral standard with *variable* amounts of common Pb
- Applications presented include U-Pb dating of apatite from >3.8 Ga gneisses from Akilia, SW Greenland
- Improves concordance in U-Pb zircon dating by enabling analysis of young, common Pb-bearing primary zircon standards